

**SILICOALUMINOPHOSPHATE (SAPO-34) GROWN ON SiC  
FOAMS AS STRUCTURED CATALYSTS FOR METHANOL  
DEHYDRATION TO DIMETHYL ETHER**

BY

MOHANNED MOHAMEDELAMIN EZZELDEN MOHAMEDALI

A Thesis Presented to the  
DEANSHIP OF GRADUATE STUDIES

**KING FAHD UNIVERSITY OF PETROLEUM & MINERALS**

DHAHRAN, SAUDI ARABIA

In Partial Fulfillment of the  
Requirements for the Degree of

**MASTER OF SCIENCE**

In

CHEMICAL ENGINEERING

May 2014

KING FAHD UNIVERSITY OF PETROLEUM & MINERALS  
DHAHRAN- 31261, SAUDI ARABIA  
**DEANSHIP OF GRADUATE STUDIES**

This thesis, written by **MOHANNED MOHAMEDELAMIN EZZELDEN MOHAMEDALI** under the direction of his thesis advisor and approved by his thesis committee, has been presented and accepted by the Dean of Graduate Studies, in partial fulfillment of the requirements for the degree of **MASTER OF SCIENCE IN CHEMICAL ENGINEERING**.



Dr. Zuhair O. Malaibari  
(Advisor)



Dr. Usamah A. Al-Mubaiyedh  
Department Chairman



Dr. Oki Muraza  
(Co-Advisor)



Dr. Salam A. Zummo  
Dean of Graduate Studies



Dr. Adnan M. Jarallah Al-Amer  
(Member)

29/5/14

Date



Dr. Mohammad Mozahar  
Hossain  
(Member)



Dr. Shaikh Abdur Razzak  
(Member)

© Mohanned Mohamedelamin Ezzelden Mohamedali

2014

## *Dedication*

I lovingly dedicate my thesis work to my mother, whose patience, sacrifice, and sincere prays of day and night make me able to succeed and achieve such milestone.

I also dedicate this thesis to the soul of my dear friend Ahmed Hassan who taught me the real meaning of patience and hope before he passed away, and for his kind wishes and prayers for which I am forever indebted.

This thesis is also dedicated with deep gratitude to my family whose encouragements and love was without a doubt vital to my success and honor.

This work is also dedicated with special thanks to my friends with whom I made nice memories and enjoyable moments that made life at KFUPM as home.

## ACKNOWLEDGMENTS

Praise and gratitude to the almighty, Allah, the most gracious the most merciful, for giving me the power to perform this work, and to his prophet Mohammed peace and blessings be upon him.

I would like to acknowledge and thank King Fahd University of Petroleum and Minerals for allowing me to pursue my master degree. Special thanks go to all the staff at the Department of Chemical Engineering for their excellence in delivering the knowledge and experience.

I would like to express my deep appreciation and gratitude to my thesis advisor Dr. Zuhair O. Maliabari and co-advisor Dr. Oki Muraza for all the help, guidance and support they provided during the course of this research. I also wish to thank my committee members Dr. Adnan J. Al-Amer, Dr. Mozahar Hossain and Dr. Abdurrazzak Shaikh for serving in my oral committee and for offering valuable comments and feedback which was crucial for the completion of this master thesis.

Also I would like to extend a warm thanks to the research excellence in nanotechnology (CENT) for allowing me to perform all the experiments and characterizations in their laboratories. Special thanks to Dr. Abbas S. Hakeem and Mr. Jerwin C. Separa for part of FE-SEM experiments. Many thanks also to Prof. Cuong Pham-Huu and his research group at the University of Strasbourg for performing the catalytic testing in their laboratories. Also, Part of the characterizations was carried out at the facilities of the ICPEES and Dr. Y. F. Liu (ICPEES) is gratefully acknowledged for performing part of the SEM analysis.

The author would like to acknowledge the funding provided by King Abdulaziz City for Science and Technology (KACST) through the Science & Technology Unit in Center of Research Excellence in Nanotechnology at King Fahd University of Petroleum & Minerals (KFUPM) for supporting this work through project No. 11-NAN2166-04 as part of the National Science, Technology and Innovation Plan. Finally I would like to thank the members of our research group at CENT, namely Mr. M. Sanhoob, Mr. Idris Bakare, Mr. Saheed Adewele, Mr. Anas Karrar, Mr. M. Hassan and Mr. Khalid Hayder for their valuable advice and nice cooperation during this research.

# TABLE OF CONTENTES

<b>ACKNOWLEDGMENTS</b> .....	<b>V</b>
<b>TABLE OF CONTENTES</b> .....	<b>VII</b>
<b>LIST OF TABLES</b> .....	<b>X</b>
<b>LIST OF FIGURES</b> .....	<b>XI</b>
<b>ABSTRACT</b> .....	<b>XIII</b>
<b>ARABIC ABSTRACT</b> .....	<b>XV</b>
<b>CHAPTER 1 INTRODUCTION</b> .....	<b>1</b>
<b>1.1 Zeolites and Zeo-type Materials</b> .....	<b>1</b>
<b>1.1.1 Historical Overview</b> .....	<b>2</b>
<b>1.1.2 Applications of Zeolite Materials</b> .....	<b>3</b>
<b>1.2 Silicoalumino Phosphate Materials (SAPOs)</b> .....	<b>4</b>
<b>1.2.1 SAPO-34</b> .....	<b>5</b>
<b>1.3 Microwave Assisted Synthesis of Zeolites</b> .....	<b>7</b>
<b>1.3.1 Microwave Assisted Growth of Zeolitic Coatings</b> .....	<b>9</b>
<b>1.4 Structured Catalysts</b> .....	<b>12</b>
<b>1.4.1 Literature on Structured Catalysts</b> .....	<b>13</b>
<b>1.4.2 Methods for Preparing Structured Catalysts</b> .....	<b>15</b>
<b>1.4.3 The Choice of the Support Material</b> .....	<b>17</b>
<b>1.4.4 Pretreatment of the Support Material</b> .....	<b>18</b>

<b>CHAPTER 2 METHANOL DEHYDRATION TO DIMETHYL ETHER.....</b>	<b>20</b>
1.5 Importance and Uses of Dimethyl Ether (DME).....	20
1.6 Methanol Dehydration to Dimethyl Ether (DME) .....	21
1.7 Catalysts Used for Methanol Dehydration to DME.....	22
1.7.1 MTD over SAPO-34 .....	23
1.7.2 MTD over Structured Catalysts .....	26
<b>CHAPTER 3 RESEARCH OBJECTIVES AND PLAN .....</b>	<b>29</b>
1.8 Research Objectives.....	29
1.9 Investigations on SAPO-34 Phase Purity.....	30
1.9.1 Conventional Hydrothermal Synthesis Method .....	30
1.9.2 Microwave Assisted Synthesis Method (MAHyS) .....	30
1.10 Fabrication of SAPO-34/SiC foam Composite .....	32
1.10.1 Effects of Synthesis Duration .....	32
1.10.2 Effects of Number of Coating Cycles.....	32
1.10.3 Effects of Support Pretreatment .....	33
1.11 Catalytic Testing for Methanol Dehydration to Dimethyl Ether.....	34
<b>CHAPTER 4 EXPERIMENTAL SETUP.....</b>	<b>35</b>
1.12 Introduction.....	35
1.13 SAPO-34 Phase Purity Studies .....	36
1.14 Fabrication of SAPO-34/SiC Foam Composite.....	40
1.15 Characterization Techniques.....	42
1.15.1 X-Ray Diffraction Analysis (XRD) .....	42
1.15.2 Scanning Electron Microscopy (SEM) .....	42
1.15.3 Nitrogen Adsorption-Desorption Experiment for BET surface Area .....	42

1.16	Methanol Dehydration to Dimethyl Ether (MTD) .....	43
<b>CHAPTER 5 RESULTS AND DISCUSSION.....</b>		<b>45</b>
1.17	Introduction.....	45
1.18	Results of SAPO-34 Phase Purity Studies.....	46
1.18.1	Hydrothermal Synthesis Method .....	46
1.18.2	Microwave Assisted Hydrothermal Synthesis Method (MAHyS) .....	49
1.19	Fabrication and Characterization of SAPO-34/SiC Foam Composite .....	50
1.19.1	Fabrication of the SAPO-34/SiC Foam Structured Catalyst .....	50
1.19.2	Effects of Microwave Irradiation Time .....	53
1.19.3	Effects of Number of Coating Cycles.....	55
1.19.4	Effects of Pretreatment with the Template Material (TEAOH) .....	60
1.20	Methanol Dehydration to Dimethyl Ether (MTD) .....	62
1.20.1	Comparison of the Dehydration Activities of Slurry and Template Seeded SAPO-34/SiC Foam Composites .....	62
1.20.2	Comparison of the Dehydration Activities of SAPO-34/SiC Composite and SAPO-34 Powder .....	66
<b>CHAPTER 6 CONCLUSIONS AND RECOMMENDATIONS .....</b>		<b>68</b>
1.21	SAPO-34 Purity Studies .....	68
1.22	Fabrication of the SAPO-34/SiC Foam Composite .....	69
1.23	Catalytic Dehydration of Methanol to DME .....	70
1.24	Recommendations and Future Work .....	71
<b>REFERENCES.....</b>		<b>72</b>
<b>VITAE.....</b>		<b>79</b>

## LIST OF TABLES

Table 1 Different Concentrations for the Synthesis of SAPO-34. Note: HY: Hydrothermal Synthesis, MW: Microwaves Assisted Synthesis.....	37
---	----

## LIST OF FIGURES

Figure 1 The Primary Unit in Zeolite Structure, Adopted from British Zeolite Organization <a href="http://www.bza.org">www.bza.org</a> .....	2
Figure 2 CHA Structure (adopted from the International Zeolite Association, IZA). .....	5
Figure 3 The Framework of SAPO-34 Showing the Atoms and One Acid Site .....	6
Figure 4 Difference in Temperature Profiles after 1 min heating in microwave (left) and in oil bath (right) adopted from [12] .....	9
Figure 5 SAPO-34 at Different Microwave Irradiation Times, (a) 2 h and (b) 4 h, Adopted from [13].....	10
Figure 6 Comparison between Conventional and Microwave Synthesis Methods .....	11
Figure 7 Catalyst Extrudated Pellets, adopted from <a href="http://www.irmatech.com">www.irmatech.com</a> .....	13
Figure 8 ZSM-5 Coated on SiC Foams as Structured Catalysts for MTO Applications from [36], (a) Optical view of foam material, (b), (c), and (d) magnified views of the composite catalyst .....	14
Figure 9 Anchorage of Zeolitic Coating (Zeolite BETA) to the Substrate Surface (SiC) adopted from [34].....	16
Figure 10 XRD Patterns of (a) Alumina support, (b) Membrane After 1st coating, and (c) after 2nd Coating [46] .....	17
Figure 11 Enhancement of Coverage by Applying Alkali Pretreatments as Reported in [47] , (a) top view, (b), (c), and (d) are side views .....	19
Figure 12 Methanol Conversion to DME on SAPO-34/ $\gamma$ -alumina at 180 °C and 1 bar adopted from [59] .....	24
Figure 13 Methanol Conversion to DME as a function of temperature adopted from [59] .....	24
Figure 14 Methanol Conversion to DME over ZSM-5, adopted from [62].....	27
Figure 15 Methanol Conversion to DME over ZSM-5/SiC foam, adopted from [62] .....	27
Figure 16 Schematics of the Experimental Plan for Phase Purity Studies .....	31
Figure 17 Stainless Steel Autoclave with PTFE Container .....	38
Figure 18 PTFE autoclave used in MAHyS .....	38
Figure 19 Microwave Reactor (MicroSynth, Milestone).....	39
Figure 20 Specially Designed Teflon Holder .....	40
Figure 21 Cross Section View of the Synthesis Reactor .....	41
Figure 22 XRD Patterns of As-synthesized Samples Using Hydrothermal Synthesis (200 °C, 24 h): Effects of $\text{SiO}_2/\text{Al}_2\text{O}_3$ .....	47
Figure 23 XRD Patterns of Samples Using Hydrothermal Synthesis (200 °C , 24 h): Effect of TEAOH Concentration .....	48
Figure 24 XRD Patterns of Samples Using Hydrothermal Synthesis (200 oC, 24 h): Effect of Water Concentration .....	48
Figure 25 XRD Patterns of As-synthesized Samples Using Microwave Irradiation (180 °C, 6 h): Effects of $\text{SiO}_2/\text{Al}_2\text{O}_3$ .....	49

Figure 26 XRD Pattern of SAPO-34/SiC Foam Composite, Synthesized at 180 °C for 6 h Microwave Irradiation .....	51
Figure 27 SEM images of (a) the SiC foam, (b) Struts of the SiC foam, (c) Struts Covered with a Continuous Layer of SAPO-34 Catalyst and (d) Magnified View of SAPO-34 Crystals .....	52
Figure 28 SEM Images of (a) SiC Foam Modified with the Precursor Solution, (b-d) SAPO-34/SiC Foam Composite After 2, 4, and 6 h Microwave Irradiation ..	54
Figure 29 XRD Patterns of SAPO-34 Samples at Different Microwave Irradiation Times .....	55
Figure 30 BET Surface Area versus Number of Coating Cycles .....	56
Figure 31 EDX Compositional Mapping After the 1 <sup>st</sup> Coating Cycle.....	56
Figure 32 N <sub>2</sub> Adsorption-desorption Experiment After the 1 <sup>st</sup> Coating Cycle.....	57
Figure 33 N <sub>2</sub> Adsorption-desorption Experiment After the 2 <sup>nd</sup> Coating Cycle .....	58
Figure 34 N <sub>2</sub> Adsorption-desorption Experiment After the 3 <sup>rd</sup> Coating Cycle .....	58
Figure 35 N <sub>2</sub> Adsorption-desorption Experiment After the 4 <sup>th</sup> Coating Cycle.....	59
Figure 36 N <sub>2</sub> Adsorption-desorption Experiment for SAPO-34 Powder Using MAHyS (180 °C, 6 h).....	59
Figure 37 Effect of Template Pretreatments of SiC foam, (a) Surface of Bare SiC foam, (b) Support Pretreated with TEAOH Solution for 1 h, (c) After 2 <sup>nd</sup> Coating Step without Template Pretreatments, (d) After 2 <sup>nd</sup> Coating Step with Template Pretreatment .....	61
Figure 38 Pore Size Distribution Determined from the Desorption Branch of the Nitrogen Isotherm on the SAPO-34/SiC Synthesized via Template (Black) and Slurry (Red) Coating .....	61
Figure 39 Methanol Conversion and Specific Dehydration Rate of the Methanol on the SAPO-34 Catalysts Synthesized by Slurry Coating (SAPO-34/SiC-S), Reaction Conditions: Atmospheric Pressure, GHSV = 4500 h <sup>-1</sup> , Catalyst Weight = 0.8 g, SAPO-34 Weight = 0.45 .....	64
Figure 40 Methanol Conversion and Specific Dehydration Rate of the Methanol on the SAPO-34 Catalysts Synthesized by Template Coating (SAPO-34/SiC-T), Reaction Conditions: Atmospheric Pressure, GHSV = 4500 h <sup>-1</sup> , Catalyst Weight = 0.8 g, SAPO-34 Weight = 0.45 .....	64
Figure 41 Conversion vs Temperature for Template coating (SAPO-34/SiC-S) .....	65
Figure 42 Conversion vs Temperature for Template coating (SAPO-34/SiC-T).....	65
Figure 43 Dehydration Activity and DME Selectivity on the SAPO-34/SiC and SAPO-34 Catalysts in a Fixed-bed Reactor, Reaction Conditions: Weight of SAPO-34 = 150 mg, Reaction Temperature = 370 °C, Atmospheric Pressure, CH <sub>3</sub> OH Concentration = 25 vol. %, Gaseous Hourly Space Velocity (GHSV) = 1000 h <sup>-1</sup> .....	67

## ABSTRACT

Full Name : Mohammed Mohamedelamin Ezzelden Mohamedali  
Thesis Title : Silicoalumino Phosphate SAPO-34 Grown on SiC Foam as Structured Catalyst for Methanol Dehydration to Dimethyl Ether  
Major Field : Chemical Engineering  
Date of Degree : May 2014

SAPO-34 layers were successfully grown on  $\beta$ -SiC foam with medium specific surface-area, using a microwave-assisted hydrothermal synthesis method (MAHyS) for applications as a structured catalyst. Preliminary investigations on SAPO-34 phase purity were conducted to select the appropriate concentrations and protocol to grow pure SAPO-34 on SiC foams. SAPO-34/SiC foams composite were obtained via a microwave-assisted synthesis route. X-ray diffraction (XRD) was used to confirm the formation of the composite. Microwave irradiation time, number of coating cycles and pretreatments with the template solution and the slurry were studied to optimize the growth and coverage of SAPO-34 crystals on the SiC foam surface. SAPO-34 crystals with cubic morphologies having 7  $\mu\text{m}$  average size were obtained after 6 h microwave irradiation treatment at 180°C. However, multi coating steps were required to obtain a full coverage of SAPO-34 crystals. Template pretreatments of the host material (SiC foams) significantly improved the loading of crystals on the support surface. Full coverage of SAPO-34 on SiC foams was obtained after 2 times of coatings, which is mostly attributed to the template layer formed on the foam surface which induced the heterogeneous nucleation on the support. The SAPO-34/SiC foam structured catalyst exhibited enhanced activity and stability in methanol dehydration to dimethyl ether, which was carried out in

a fixed bed reactor. The supported zeolite displays the same intrinsic activity compared to the powder zeolite and the dehydration activity obtained on the template coated catalyst, SAPO-34/SiC-T, is higher than the one obtained on the slurry coated catalyst, SAPO-34/SiC-S

## ملخص الرسالة

الاسم الكامل: مهند محمد الأمين عزالدين محمد علي

عنوان الرسالة: طلاء فوسفات السيليكا ألومينا 34 على كربونات السيلكون الرغوية و إستخدامها كحفاز مركب في تفاعل نزع الماء من الميثانول لتكوين ثنائي ميثيل الإيثر

التخصص: الهندسة الكيميائية

تاريخ الدرجة العلمية: مايو 2014

تم بنجاح عمل طبقة من SAPO-34 على سطح كربونات السيلكون الرغوية ذات مساحة السطح المتوسط باستخدام التحضير بواسطة المايكرويف و إستخدام هذا التركيب كعامل حفاز في تفاعل نزع الماء من الميثانول لتكوين ثنائي ميثيل الإيثر. تم عمل دراسات أولية لدراسة نقاء SAPO-34 و ذلك لإختيار التراكيز المناسبة للحصول على SAPO-34 نقي و طلائه على سطح كربونات السيلكون الرغوية. مركب SAPO-34/SiC المنتج بواسطة المايكرويف تم تأكيد إنتاجه بإستخدام تجربة إنحراف الأشعة السينية. تمت أيضا دراسة تأثير زمن التحضير في المايكرويف، عدد مرات التحضير و عمليات معالجة مبدئية لسطح كربونات السيلكون الرغوية بإستخدام محلول العامل الحفاز و محلول العامل المساعد للتشكيل. تم الحصول على بلورات SAPO-34 بحجم 7 مايكرون بعد إشعاع مايكرويف لمدة 6 ساعات في درجة حرارة 180 درجة مئوية. إعادة عملية التحضير ضرورية للحصول على تغطية كاملة لسطح كربونات السيلكون الرغوية. المعالجة المبدئية لسطح كربونات السيلكون الرغوية أدت لتحسين كمية البلورات المطلوبة و تم تحقيق تغطية كاملة لسطح كربونات السيلكون الرغوية بعد إعادة عملية التحضير مرتين متتاليتين و يعزى هذا التأثير للطبقة التي تكونت فوق سطح كربونات السيلكون الرغوية قبل تكوين البلورات و التي أدت لزيادة كمية البلورات المتكونة فوق سطح كربونات السيلكون الرغوية أكثر من الكمية المتكونة في المحلول. مركب SAPO-34/SiC تم إختباره في تفاعل نزع الماء من الميثانول لتكوين ثنائي ميثيل الإيثر و قد أبدى أداء عاليا و إستقرارية كبيرة داخل المفاعل. أيضا الحفاز المركب من بلورات SAPO-34 و كربونات السيلكون الرغوية أعطت نفس الأداء مقارنة ببلورات SAPO-34 المستخدمة في شكل مسحوق. كما أن طريقة معالجة السطح بمحلول العامل المساعد للتشكيل أبدت أداء أفضل من المعالجة بمحلول العامل الحفاز في المفاعل.

# CHAPTER 1

## INTRODUCTION

### 1.1 Zeolites and Zeo-type Materials

Zeolites and zeo-type materials are microporous crystalline solids that are used for possessing different crystal structures. Zeo-type materials are available naturally as minerals all over the world. However, others are produced synthetically, and exist in commercial scale for specific applications, or produced on lab scales to understand their properties and multiple uses.

Applications of zeo-type materials as catalysts in a variety of industries are well known. Zeolites are having global demand of several million tonnes annually ([www.bza.org](http://www.bza.org)). Examples of applications of zeolites are petrochemical industries, construction, separation of gases and environmental uses.

The basic unit cell of zeo-type materials is made of an atom linked to four oxygen atoms. This building unit is well known as tetrahedra, which is connected to the neighboring unit through an oxygen atom, as can be seen in Figure 1, to form different framework structures. The primary unit in zeolites is  $\text{SiO}_4$  and  $\text{AlO}_4$  tetrahedras, while some zeo-type materials are made of  $\text{SiO}_4$ ,  $\text{AlO}_4$  and  $\text{PO}_4$  as in the microporous silicoalumino phosphates known as SAPOs.

One of the important features of zeolites is the framework structure resulted from the connection between the tetrahedras. This framework may form channels, cavities and cages with molecular dimensions ranging from 3 to 30 Å. This regular porosity allows zeolites to act as shape-selective catalyst, to separate molecules based on size and shape.

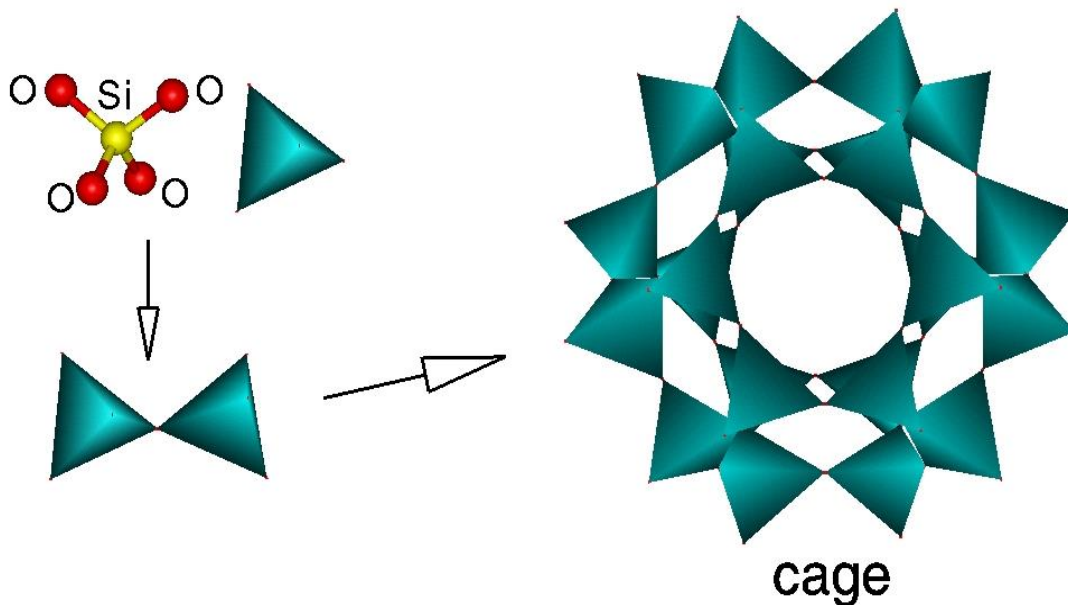


Figure 1 The Primary Unit in Zeolite Structure, Adopted from British Zeolite Organization [www.bza.org](http://www.bza.org)

### 1.1.1 Historical Overview

The name zeolite is originated from the Greek “zeo” which means to boil, and “lithos” which means stones, as it releases water upon heating. The year 1756 witnessed the discovery of the first zeolite mineral (Stilbite), discovered by the Swedish scientist Cronstedt [1].

The exact date of synthetic zeolites is not clear, because of difficulties in reproducibility and the lack of powerful characterization techniques. However, Barrer in 1945 reported

the first group of zeolite materials, the molecular sieve materials [2]. After the work of Barrer, the industrial community became more interested in the synthesis of zeo-type materials, and their application in different fields.

The use of zeolites in catalysis is started in 1950s [3] especially in oil refining and petrochemical industries, utilizing their shape selectivity in separation and catalyzing reactions. The first zeolite material used in catalytic applications was the Faujasites, FAU [4]. Nowadays more than 218 framework of zeo-type materials have been discovered [www.iza-structure.org](http://www.iza-structure.org).

### **1.1.2 Applications of Zeolite Materials**

The channels and cavities in zeolites frameworks provide a selective surface area for chemical reactions to take place. Moreover, the ion exchange of zeolites and zeo-type materials to create hydrogen form of zeolites, give rise to strong acid sites within the zeolite framework. Different kinds of reactions can occur on these sites for instance cracking of crude oil and isomerization reactions.

Metal impregnation into the zeolite frameworks enables oxidation and reduction reactions to take place such as NO<sub>x</sub> decomposition on copper-zeolite catalysts.

The unique microporosity of zeo-type materials, where the size and shape of the microporous structure along with the chemical properties such as acidity, play the main role in controlling the activity, selectivity and stability of the zeolite in different reactions. Therefore, great attention has been paid to tune the properties of zeo-type materials in order to investigate feasibility of conducting new catalytic reactions and improve the performance of some existing reactions.

Zeolites have been used as molecular sieves to benefit from their ability to selectively adsorb some molecules and allow the others to pass through, depending on the size and shape of the molecules. For example, separation of para-Xylene isomer by silicalite is one of the famous applications.

Introducing different cations into the zeolite framework affect their affinity for water and thus their use as desiccants and in the separation of gases based on certain interactions with the metal ions. On the other hand, some hydrophobic zeolites are used to separate organic materials.

## **1.2 Silicoalumino Phosphate Materials (SAPOs)**

The group of molecular sieve materials comprises zeolites (aluminosilicates), microporous silica, alumina phosphate and silicoalumino phosphates. The SAPOs possess properties that enabled them to be widely used in adsorption, gas separation and catalysis. Up to now, there are 13 discovered frameworks that belong to SAPO group of molecular sieves [5], including SAPO-34 (CHA), SAPO-37 (FAU), SAPO-5 (AFI) and SAPO-18 (AEI). Silicoalumino phosphates, SAPOs are prepared via hydrothermal synthesis route in a range of temperature from 100 to 200 °C, from a gel containing sources of Si, Al, P and a structure directing agent material.

Aluminophosphate (AIPO) and silicoaluminophosphate (SAPO) molecular sieves were originally discovered by Union Carbide in 1980s [6]. AIPOs and SAPOs possess wide range of framework structures. The frameworks of AIPO molecular sieves are electrically neutral with no catalytic activity. The incorporation of silicon into AIPOs framework to form SAPOs, results in a negative charge which is neutralized by the proton remained

after the decomposition of the structure directing agent in the calcination process producing hydroxyl groups as Bronsted acid sites [5].

### 1.2.1 SAPO-34

During the past decade, SAPO-34 with a CHA structure and a small pore size (Figure 2) has received great attention and been recognized for the selective conversion of methanol to light olefins. Several modifications of SAPO-34 physico-chemical properties are described for instance, composition [7], crystal size [8], and metal incorporation [9].

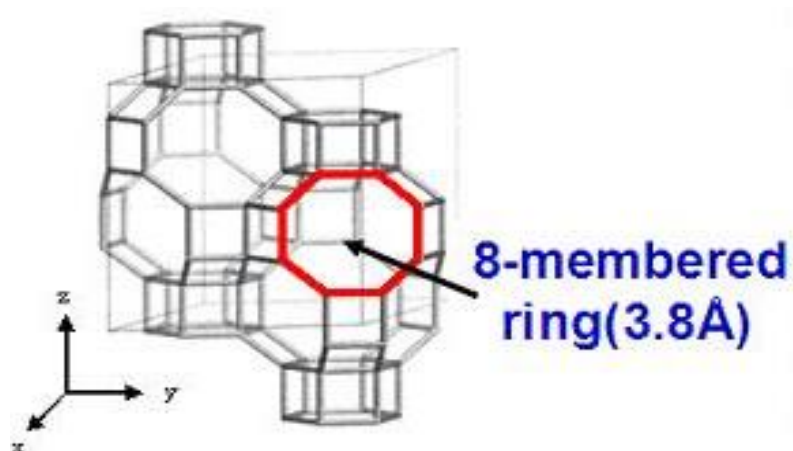
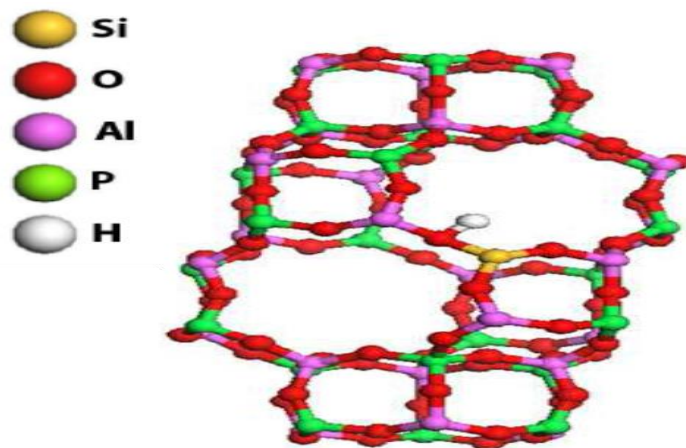


Figure 2 CHA Structure (adopted from the International Zeolite Association, IZA).

The chabazite structure of SAPO-34 is made of cages of about 1 nm, however, the channels between these pores is much smaller (only 0.38 nm), which means that only molecules with molecular diameter smaller than 0.38 nm can pass through the pores and that bigger molecules will be enclosed inside the cages. Figure 3 shows the structure of

one unit in the CHA framework of SAPO-34, where the incorporation of silica result in a formation of one acid site.



**Figure 3 The Framework of SAPO-34 Showing the Atoms and One Acid Site**

### 1.3 Microwave Assisted Synthesis of Zeolites

As discussed earlier that the synthesis of SAPO-34 catalyst was achieved by the reaction of the constituents of the gel mixture prepared by mixing Si, Al and P sources plus a structure directing agent. This mixture was allowed to undergo crystallization process at elevated temperatures, which took place either in conventional ovens or in special microwave irradiation ovens. Different works were reported for the synthesis of SAPO-34 catalysts and investigating the effects of heating methods [10].

Recently, the application of high-speed synthesis with microwave irradiation has gained great attention. The first application of microwave mediated synthesis method in accelerating the synthesis of organic materials was reported by Gedye and co-workers in 1980s [11]. Most of the early uses of microwave assisted synthesis were in small domestic microwaves, therefore there were different problems: the availability of temperature and pressure controllers, flammability of some materials under microwave radiation, and the absence of a mature understanding of the microwave heating mechanism. A great increase in the applications of microwave in synthesis has taken place as a result of the manufacturing of microwave instruments for synthetic application. Microwave assisted hydrothermal synthesis (MAHyS) techniques have many advantages other than reducing the synthesis time, such as increasing the throughput, avoiding side reactions and reduce the crystal size and uniformity of crystals. The basic theory behind microwave synthesis relies on “dielectric heating”, which is based on the idea that a material in the synthesis mixture absorbs the microwave irradiations and efficiently

converts this energy into heat. Figure 4 shows the difference between conventional and microwave heating readings and profiles. It can be clearly observed that microwave heated the whole mixture almost simultaneously, while the conventional heating shown temperature variations between the external surface adjacent to the oil bath and the liquid inside the vessel.

Two distinct mechanisms are reported for the microwave heating, the di-polar polarization and the ionic conduction. When microwave irradiation hits the sample with the specified frequency, it leads to ions to align in the corresponding electrical zone, and as the source frequency oscillates, the ion starts to relocate with the alternating applied energy. This movements of the ion, result in a release of energy in a form of heat, which eventually transfer to the synthesis mixture. The heat release of a material differs from other materials depending on many factors related to its electric properties mainly the so called, the loss factor.

The acceleration property of the microwave irradiation is normally related to the attaining the reaction temperature in very short duration as compared to conventional heating methods where, heat transfer resistance takes place and slow down the time required to reach the assigned temperature.

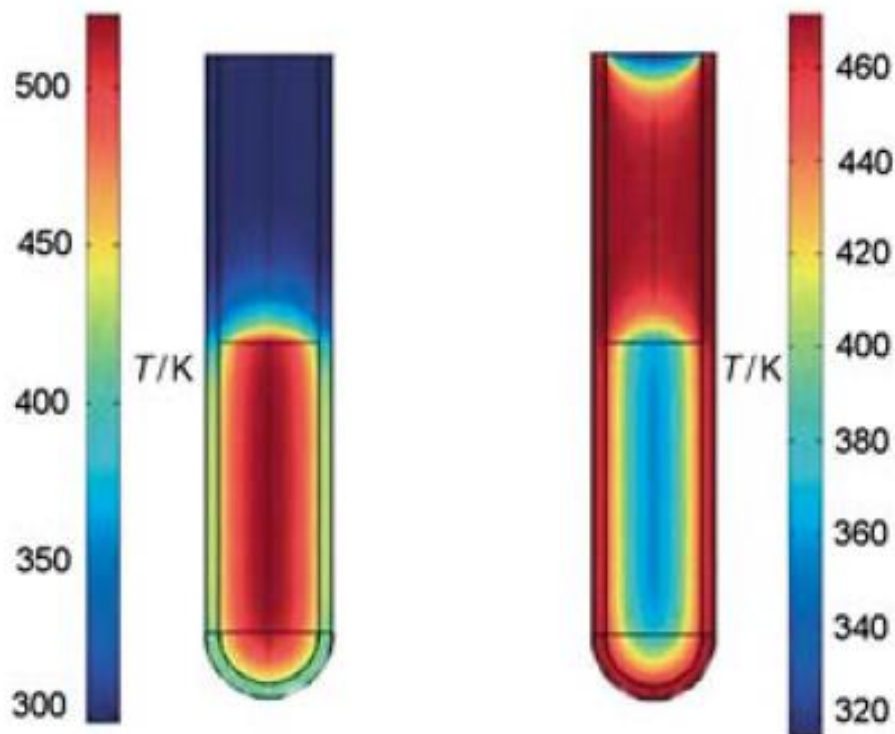


Figure 4 Difference in Temperature Profiles after 1 min heating in microwave (left) and in oil bath (right) adopted from [12]

### 1.3.1 Microwave Assisted Growth of Zeolitic Coatings

Recently, microwave assisted hydrothermal synthesis (MAHyS) has been applied for the preparation of thin films of zeolitic coatings on supports. Microwave mediated synthesis has shown remarkable increase in crystallization rates and furthermore, produced different morphologies, loadings and orientations, leading to great enhancements in their intended applications in membrane separation and structured catalysts.

Figure 6 shows the observed differences in growth and crystals size between the conventional and microwave heating methods. Heterogeneous nucleation is favorable in microwave assisted synthesis methods, with homogeneous growth of small size crystals,

on the other hand, conventional heating favors the homogeneous growth and resulted in larger crystal sizes.

Liu et al [13] has studied the growth of SAPO-34 on  $\alpha$ -Al<sub>2</sub>O<sub>3</sub> substrates using microwave energy for different reaction times and they obtained SAPO-34 with cubic morphologies after 4 h microwave irradiation as shown in Figure 5.

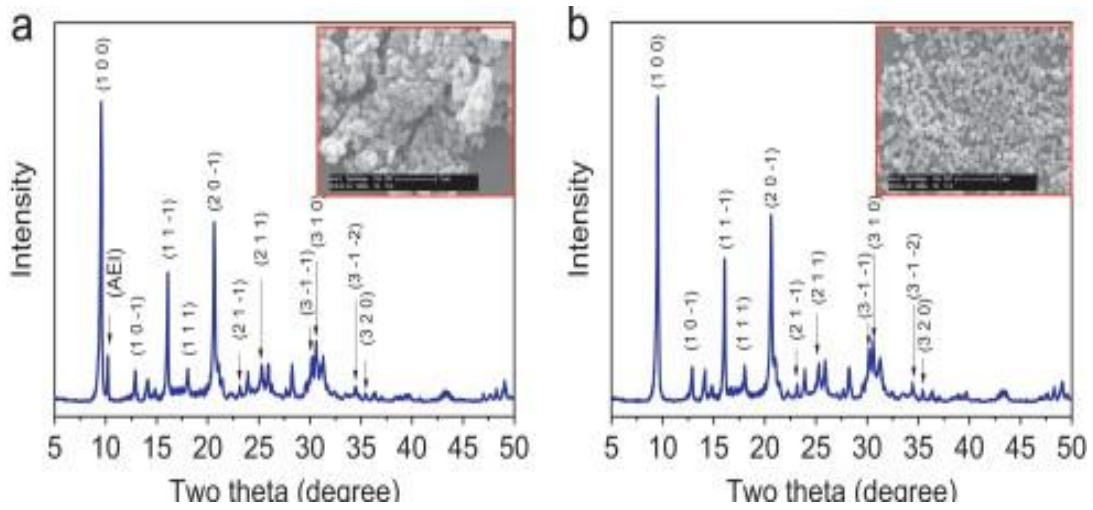
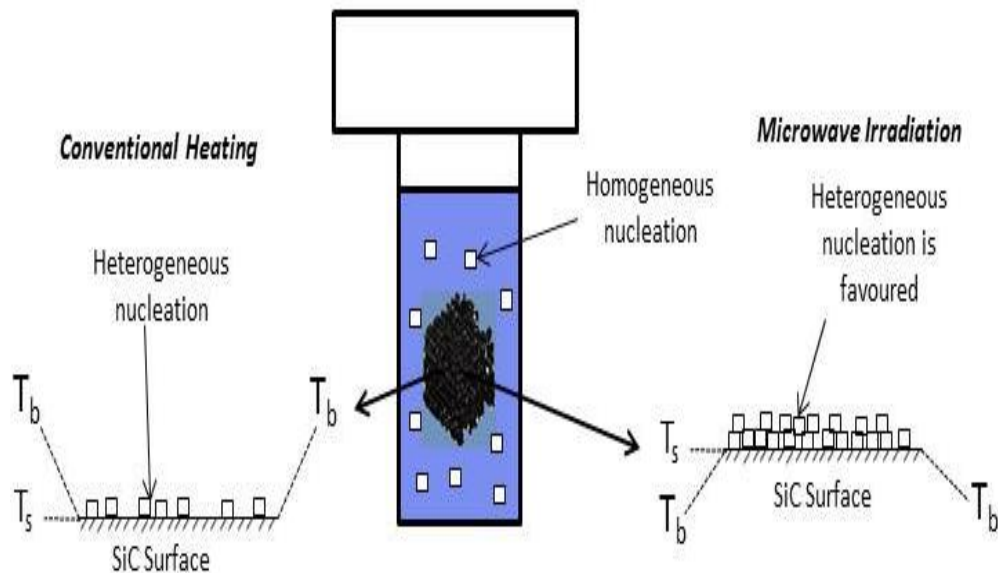


Figure 5 SAPO-34 at Different Microwave Irradiation Times, (a) 2 h and (b) 4 h, Adopted from [13]



**Figure 6 Comparison between Conventional and Microwave Synthesis Methods**

Caro and his group in 1995 reported the preparation of aluminophosphate  $\text{AlPO}_4\text{-5}$  crystals on nickel grids and their use as membranes [14]. After this work many articles have been published targeting microwave synthesis of zeolitic coatings, [15].

Microwaves could be used in most of the techniques used for zeolitic coatings, and mostly used for the in-situ hydrothermal growth [16-18] and secondary growth methods [19-21].

## 1.4 Structured Catalysts

Structured catalysts are class of composite materials, made by coatings of zeolitic materials on substrates, either through physical or chemical bonding. These composite materials are used in different applications comprising catalysis, adsorption and membranes [22].

Remarkable advances in the synthesis and in the application of structured catalysts had been achieved during the last decades, particularly investigating a variety of support materials, preparation methods, and visibility of preparing oriented films. Recently, the application of structured catalysts is gaining more attention, with numerous zeolite/substrate composite materials developed, for a wide range of applications. Structured catalysts are promising alternatives to fixed bed catalytic reactors (see Figure 7) providing several considerable aspects: enhanced hydrodynamic, better heat and mass transfer and easy access to the catalyst active centers.

For instance, the elevated heat conductivities of the substrate materials used in structured catalyst is beneficial for attaining isothermal conditions in highly exothermic reactions via accelerating heat transfer process and providing better temperature control.

Great enhancement in both mass and heat transfer could be obtained in the structured catalysts through the large interfacial surface area between the coated zeolite and the support surface, Moreover, the presence of chemical interaction between the substrate and the coated zeolite significantly enhance the heat transfer process [23].



Figure 7 Catalyst Extruded Pellets, adopted from [www.irmatech.com](http://www.irmatech.com)

#### 1.4.1 Literature on Structured Catalysts

Zeolites have been successfully grown on different host materials including stainless-steel [24, 25], honeycombs [26, 27], glass [6] and ceramic foams [28-30], and most of the studied cases proved the superior catalytic activity of the supported catalysts over the unsupported one. Thorough review on the uses of composite catalysts is reported in [31].

Among the support materials used, the SiC possesses several advantages such as good intrinsic thermal conductivity, medium to high surface area (10 to 100 m<sup>2</sup>/g), large pores, controlled macroscopic shape, and chemical inertness. The high chemical inertness of the SiC allows it to be efficiently employed in the structured zeolite synthesis without facing problems of chemical dissolution during the course of the hydrothermal synthesis. SiC foams are promising substrates for zeolite growth, and have been intensively studied for their chemical stability, mechanical strength and high thermal conductivity [32]. Coatings of different zeolites on SiC foams are reported for instance ZSM-5 [33], Beta zeolite [34]

and silicalite [35], and has shown superior performances in certain reactions [34, 36]. The advantages of using SiC foam structure are the following: (i) high external surface area which significantly improve the external mass transfer rates, (ii) high porous structure which leads to an extremely low pressure drop even at high gaseous space velocity, and (iii) the foam structure plays a role of static mixer allowing the good mixing of the gaseous or liquid reactant through the foam. Figure 8 shows SEM images of ZSM-5 on SiC foams.

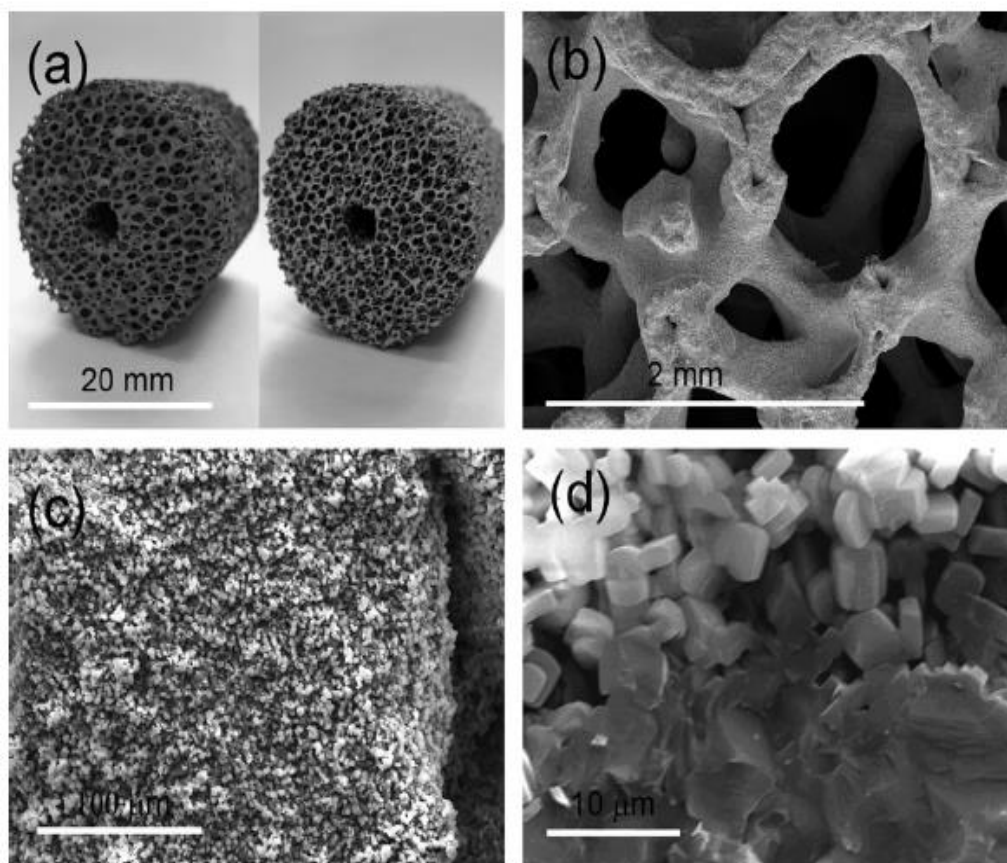


**Figure 8 ZSM-5 Coated on SiC Foams as Structured Catalysts for MTO Applications from [36], (a) Optical view of foam material, (b), (c), and (d) magnified views of the composite catalyst**

## 1.4.2 Methods for Preparing Structured Catalysts

Different methods have been developed for the fabrication of zeolite layers on solid surfaces including dip-coating [37, 38], slurry-coating [39-41] and direct in situ synthesis on supports [23, 29, 42-45].

In the slurry-coating method, zeolite films are achieved by spraying the zeolite material on the support surface, and consequently removing the liquids via drying process. The main drawback of this method is the poor Van der Waals interaction between the coated film and the support surface.

However, in wash coating technique, a binder is added to the zeolite solution before allowing spraying over the host support. This binder reduces the accessibility of the active sites of the crystals. In addition, this method produces crystals with random distribution and orientation.

The direct in situ growth on the support has advantage over the dip and slurry coating because it yields in a full coverage of oriented crystals with strong adherence to the support surface. Presence of chemical bonding between the support surface and the coating material through the hydroxyl groups as shown in Figure 9 is beneficial from the mass and heat transfer viewpoints.

There are different growth mechanisms for the zeolitic layers on substrate surfaces. Direct growth of zeolite films on the support surface (heterogeneous nucleation), which usually takes place in diluted gel mixtures and the mass transfer of the active materials from the liquid phase to the support surface is the controlling step. Moreover, this mechanism results in the formation of small crystals with narrow size distribution.



tight membrane. Figure 10 below shows XRD patterns of the as-synthesized SAPO-34 membrane after different synthesis times. It can be clearly observed that the peak intensities of SAPO-34 increased with the increase of coating cycles, while the intensities of the substrate were decreasing.

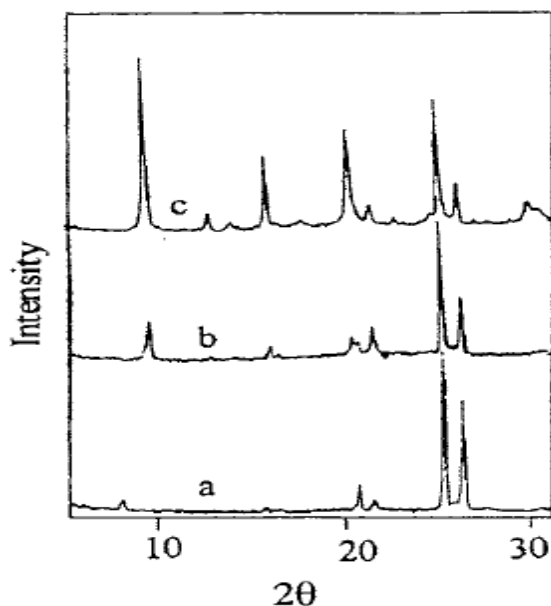


Figure 10 XRD Patterns of (a) Alumina support, (b) Membrane After 1st coating, and (c) after 2nd Coating [46]

### 1.4.3 The Choice of the Support Material

The right choice of the support material for structured catalyst is based on many factors such as, chemical stability in the synthesis environment of the zeolitic coating, mechanical and thermal properties required for the specific application and the surface hydrophilicity. For instance, the high temperature application requires the use of a substrate material with special melting point and thermal conductivities such as Aluminum and Copper. Moreover, if the mechanical strength is required then quartz and

Nickel could be used. However, for isothermal reaction applications, silicon could be used to provide efficient removal of heat from the reaction media.

Metals as support material are incompatible with some applications involving fabrication of some chemicals. Glass could be widely used in applications at lower temperatures such as preparation of liquid materials.

#### **1.4.4 Pretreatment of the Support Material**

Pretreatment of the support surface prior to the direct growth of zeolitic coatings has shown great improvements in different parameters that significantly affect the properties of the composite catalyst.

Surface modification of the substrate material is aimed mainly to activate the support surface and enhance the surface hydrophilicity in order to host the zeolitic coating. This in effect increases the sites where crystals nucleation and growth takes place. Furthermore, surface pretreatments considerably affect the stability of the substrate material in the gel mixture during the synthesis process. Surface pretreatments also, affect the coverage and loading of the zeolite layers grown on the support and significantly improve the anchorage and the bonding of the zeolite film to the support surface [47].

Different kinds of treatments are reported in literature, for example heat pretreatments at elevated temperatures is reported for SiC foam supports in order to create a nano-layer of SiO<sub>2</sub> on the surface to act as anchoring centres for zeolite crystals [48].

Alkali pretreatments of support materials has also shown giant enhancement in the enhancement of loading and anchorage of MCM-22 crystals on the surface of SiC foam.

Figure 11 shows a proof for this enhancement.

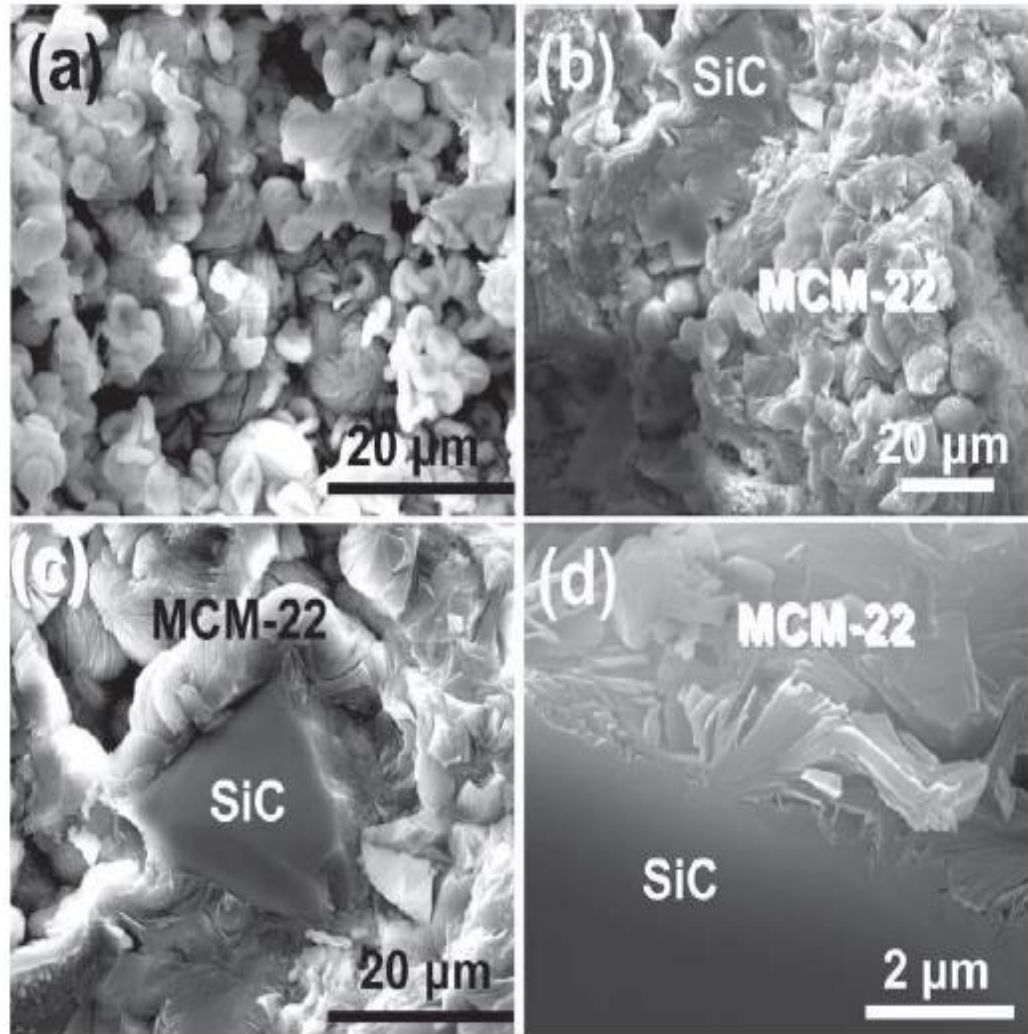


Figure 11 Enhancement of Coverage by Applying Alkali Pretreatments as Reported in [47] , (a) top view, (b), (c), and (d) are side views

## CHAPTER 2

### Methanol Dehydration to Dimethyl Ether

#### 1.5 Importance and Uses of Dimethyl Ether (DME)

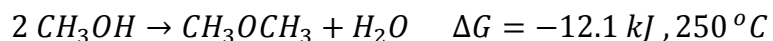
Dimethyle ether (DME) is an organic compound with a molecular formula ( $\text{CH}_3\text{OCH}_3$ ) possessing the following properties: non-corrosive, non-toxic, colourless and environmentally friendly material. Dimethyl ether (DME) is the simplest ether with no carbon-carbon bond.

Dimethyle ether (DME) has gained considerable attention over the last decades because of its potential application as a fuel that is capable for replacing the existing diesel fuels which contributes in the air pollution and leading to severe environmental problems.

It is also widely used to replace the existing cooling units that are fueled by chlorofluorocarbons, which is proven to harm the environment and cause ozone layer depletion, therefore globally banned. Another indirect application of dimethyl ether is the use of DME as a feed for the production of light olefins [49]. It can also be reformed to form  $\text{H}_2$  for fuel cells [50].

## 1.6 Methanol Dehydration to Dimethyl Ether (DME)

Dimethyl ether (DME) has been traditionally produced from methanol which is already been produced from syngas, through a proven technology. The catalytic conversion of methanol into dimethyl ether on solid acids is believed to take place on both Lewis and Bronsted acid sites [51]. The reaction scheme below represents the dehydration of methanol to dimethyl ether



Several solid-acid catalysts have been utilized in the methanol to dimethyl ether (MTD) reaction, comprising alumina, ZSM-5, Mordenite and SAPOs [52]. Many studies have been dedicated in literature to understand the mechanism and kinetics of this reaction on solid acid catalysts. However, the mechanism of the dehydration process varies depending on the catalyst used.

## 1.7 Catalysts Used for Methanol Dehydration to DME

According to Bandiera and co-workers [53], where they studied the MTD reaction on dealuminated H-Mordenite catalyst, they proposed a reaction scheme based on Langmuir-Hinshelwood mechanism where two molecules of methanol are adsorbed on Lewis and Bronsted basic sites respectively and reacts on the surface of the catalyst to produce DME. Kubelkova and co-workers proposed another mechanism for MTD where they used ZSM-5 and HY as catalysts. They suggested that only one methanol molecule is adsorbed on the Lewis acid site which is further react to release water and form a methoxy group on the surface as follows.

One of the major problems that need to be addressed in the methanol dehydration to dimethyl ether is the catalyst deactivation which is mostly associated with the formation of hydrocarbons which is subsequently converted to coke in the presence of strong acid sites or at high reaction temperatures. Attempts have been made to search for catalysts with mild (or weak) acidity that work at low temperatures.

Thorough investigation has been made on the tuning of the acidity of catalysts material used in MTD reaction, for instance Kim et al [54] studied the modification of ZSM-5 to enhance the performance and stability in MTD reaction. Also, Khandan and co-workers [55] studied different modifications on Mordenite, Ferrierite and Beta in order to adjust the acidity and improve the activity, selectivity and stability in MTD reaction.

However, the use of aluminophosphates and silicoaluminophosphates molecular sieves in the conversion of methanol to dimethyl ether is potential for methanol dehydration to

dimethyl ether as they have weaker acid sites as compared to other zeolites; hence they are expected to exhibit superior performances in MTD. Few studies have been performed in literature addressing the use of  $\gamma$ -alumina with phosphorous and  $\text{AlPO}_4$  in methanol dehydration to dimethyl ether [56] and [57] respectively.

Weili and co-workers [58] have studied the use of AlPO-5, AlPO-11, AlPO-41 and their corresponding silicon substituted materials SAPO-5, SAPO-11 and SAPO-41 for methanol dehydration to dimethyl ether with focus been on the effect of acid sites and temperature. A yield of about 85% at 100% DME selectivity was obtained for SAPO-11 at 250 °C.

### **1.7.1 MTD over SAPO-34**

The methanol dehydration to dimethyl ether over SAPO-34 molecular sieve has been studied by Grigore Pop and co-workers [59], where the SAPO-34 catalyst has been blended with alumina as binding agent. Reaction is performed in the temperature range between 100 to 250 °C and pressure from 1 to 10 bar. This composite catalyst exhibited enhanced catalytic activity and selectivity in MTD reaction, with catalyst durability up to 50 h. Figure 12 below reveal the catalyst stability with a conversion of about 80% and stability up to 50 h. Also the effect of temperature on conversion is shown in figure 13.

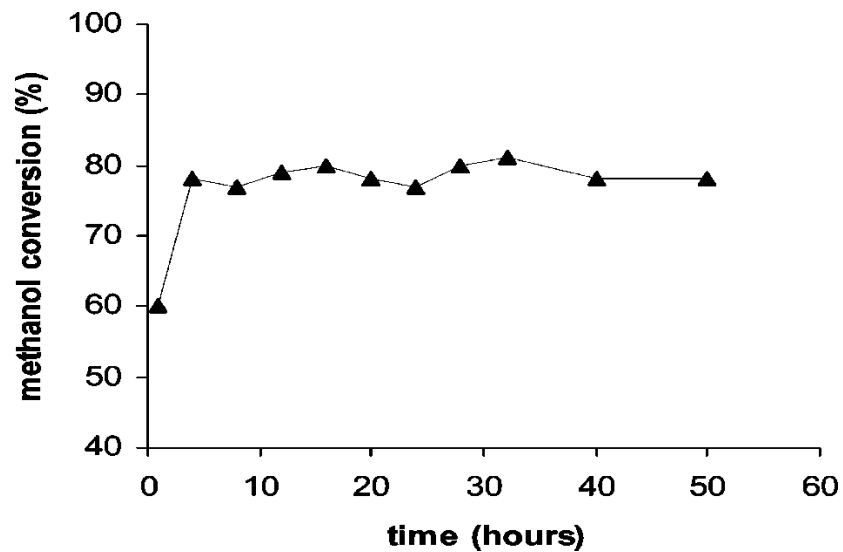


Figure 12 Methanol Conversion to DME on SAPO-34/ $\gamma$ -alumina at 180 °C and 1 bar adopted from [59]

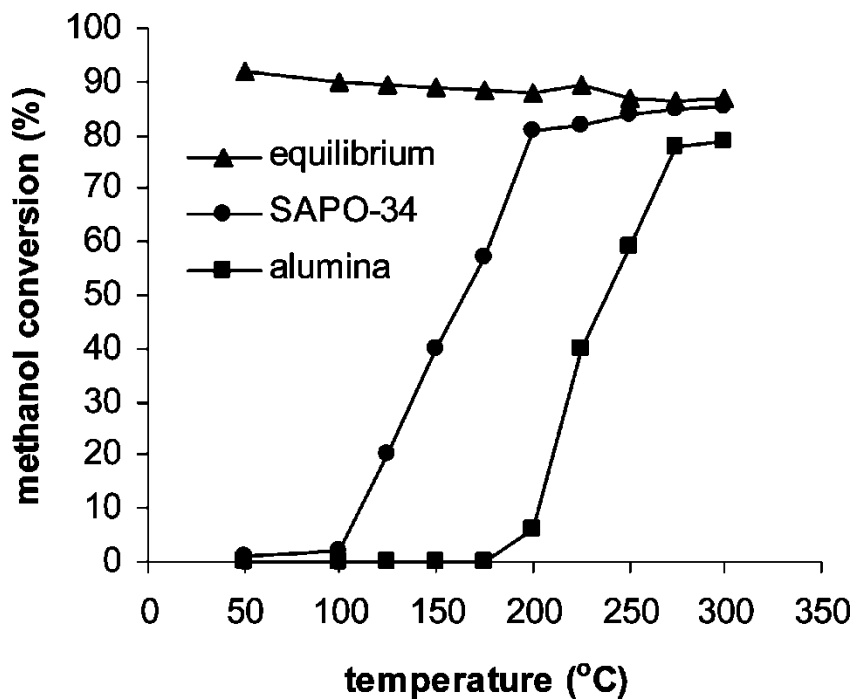


Figure 13 Methanol Conversion to DME as a function of temperature adopted from [59]

The first work addressing the kinetic modeling of methanol dehydration to dimethyl ether on SAPO-34 catalyst was conducted by Pop et al [59] in 2009. They performed catalytic evaluation of the catalyst in a laboratory fixed bed reactor operating at temperature from 100 to 200 °C, pressure from 1 to 10 bar, and liquid methanol space velocity between 2 to 5 h<sup>-1</sup>. The catalyst was prepared in an extrudated pellets form by mixing with  $\gamma$ -alumina binders, and operated at feed flow rates enough to overcome the external diffusion limitations.

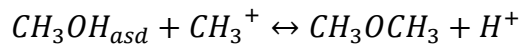
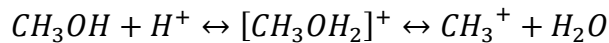
Among the all published kinetics models, the expression given by Lu and co-workers [60] where two bronsted acid sites participates in the MTD reaction- it gave the most adequate rate model as shown below.

$$r_E = \frac{k \left[ \frac{P_M^2}{P_W} - \frac{P_E}{K_P} \right]}{(1 + K_M P_M + K_W P_W)^2}$$

Where

M, W, and E represents methanol, water and DME respectively, and K<sub>P</sub> is the equilibrium constant.

The proposed mechanism by Lu et al includes the following steps:



## 1.7.2 MTD over Structured Catalysts

The use of structured catalysts has proved an impressive enhancement in several areas of applications. Structured catalysts have been widely used for the conversion of methanol. For instance Cu/ZnO catalyst impregnated into catalyst paper has been utilized as a composite catalyst for the steam reforming of methanol, and has shown superior performances to the conventional powdered catalysts [61]. Moreover, metal-supported catalysts have also been used for hydrogen production from methanol via steam reforming process and have significantly improved the heat transfer during the reforming reaction.

However, the first work on the use of structured catalysts from methanol dehydration to dimethyl ether was reported by Cuong et al in 2008 [62] using ZSM-5 as an active phase and  $\beta$ -SiC foam as support material. Catalytic activity and stability was compared for both the supported and the powder ZSM-5. Reaction was performed in atmospheric pressure and a temperature of about 270 °C in a fixed bed reactor. Higher initial conversion of methanol on the powder ZSM-5 was observed (Figure 14), which dropped dramatically after 2 h indicating deactivation of the catalyst by the coke formed on the acid sites. On the other hand, ZSM-5/SiC composite has shown stable performance with an average conversion of 60% (Figure 15).

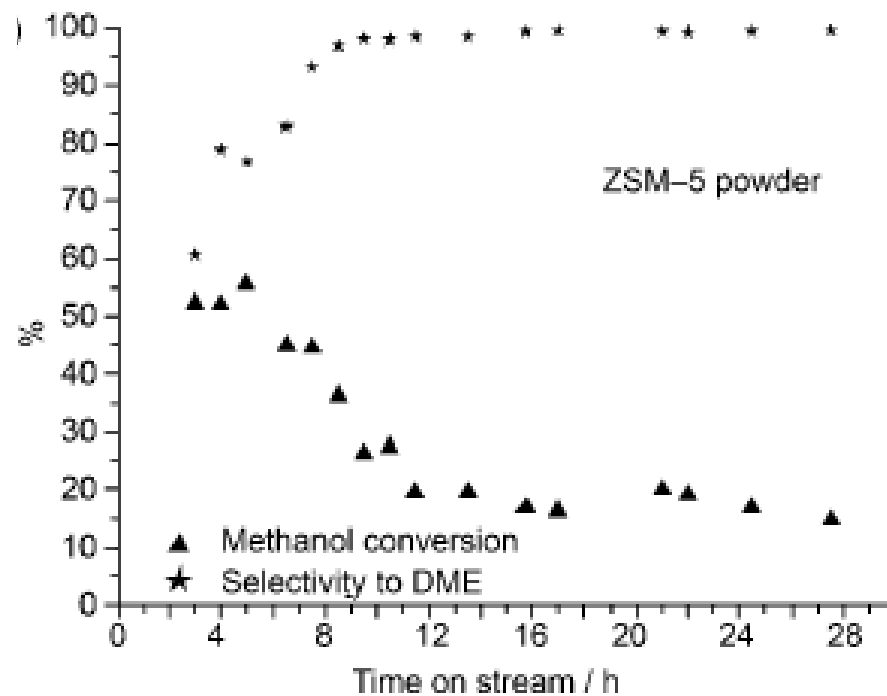


Figure 14 Methanol Conversion to DME over ZSM-5, adopted from [62]

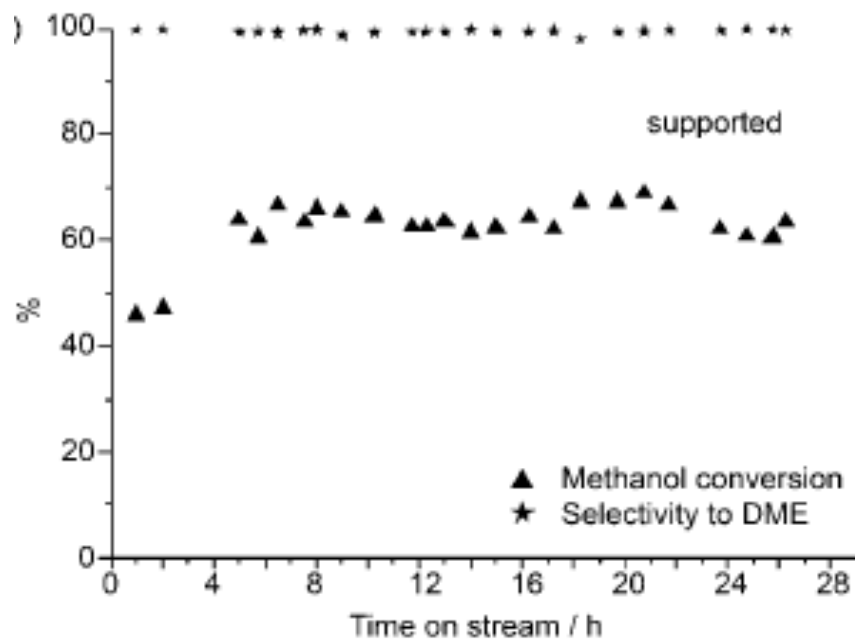


Figure 15 Methanol Conversion to DME over ZSM-5/SiC foam, adopted from [62]

Another similar work is also reported by Liu et al in 2011 [63] where again ZSM-5/SiC composite was used for MTD reaction and the same positive effect of using structured catalyst in catalyzing MTD reaction is proved

## CHAPTER 3

### RESEARCH OBJECTIVES AND PLAN

#### 1.8 Research Objectives

The objective of this study was to investigate the direct insitu growth of silicoalumino phosphate zeo-type material, SAPO-34 with CHA structure on medium surface area  $\beta$ -SiC foams, and their application as structured catalysts for methanol dehydration to dimethyl ether (DME). The goals of this research could be divided into the following points:

1. Fabricate the novel SAPO-34/SiC foam structured catalyst.
2. Determine the appropriate formulations to produce pure SAPO-34 prior to the growth on SiC foam.
3. Control the growth of SAPO-34 crystals on SiC foams.
4. Study the catalytic activity and selectivity of the SAPO-34/SiC composites and the SAPO-34 powder (fixed bed).
5. Comparison of the dehydration activity of SAPO-34/SiC composites prepared with template pretreatment and slurry pretreatments at different temperatures.

Detailed plan of the work done in this thesis containing different sub-objectives is provided in the following sections.

## **1.9 Investigations on SAPO-34 Phase Purity**

Prior to growth of SAPO-34 on SiC foams, thorough investigations were conducted to identify the concentrations at which pure SAPO-34 is obtained. Both microwave assisted hydrothermal synthesis (MAHyS) and conventional hydrothermal synthesis methods were utilized. Effects of template concentration, Si/Al ratio and water concentrations were studied on both methods. XRD was used in the identification of the present phases, and to evaluate the effect of the different parameters on crystallinity. Figure 16 below shows schematics of the experimental plan for this part.

### **1.9.1 Conventional Hydrothermal Synthesis Method**

In this work, different synthesis parameters were varied using the conventional hydrothermal synthesis methods in order to study the effects of these parameters on SAPO-34 phase purity.

SiO<sub>2</sub>/Al<sub>2</sub>O<sub>3</sub> ratio, template concentration (tetraethyl ammonium hydroxide, TEAOH) and H<sub>2</sub>O/Al<sub>2</sub>O<sub>3</sub> ratio of the starting solution was varied and four samples were prepared from each parameter variation. XRD was used to study the effect of these parameters on the different phases exist and the crystallinity of the samples. Emrani and co-workers [64] have studied the effect of synthesis parameters on SAPO-34 crystal size, morphology and crystallinity.

### **1.9.2 Microwave Assisted Synthesis Method (MAHyS)**

The use of microwave mediated synthesis method was investigated in this report, and the variation of two parameters was conducted to obtain appropriate formulation that gives

pure SAPO-34 with MAHyS method. The parameters are namely, the effect of  $\text{SiO}_2/\text{Al}_2\text{O}_3$  ratio of the starting synthesis mixture, and the effect of crystallization time.

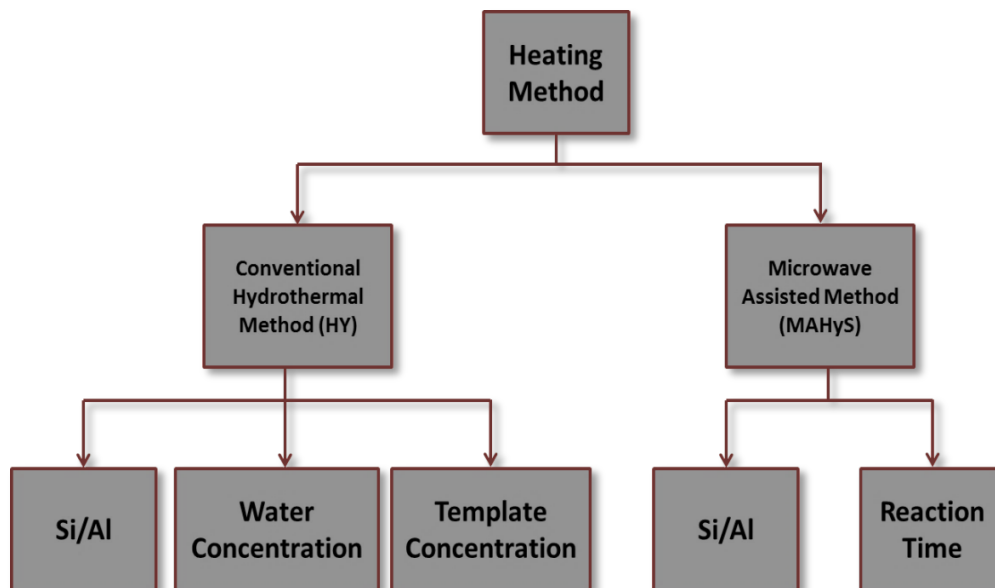


Figure 16 Schematics of the Experimental Plan for Phase Purity Studies

## **1.10 Fabrication of SAPO-34/SiC foam Composite**

Using the results from part 1 (SAPO-34 phase purity studies), with the gel concentrations and the appropriate operating conditions, SAPO-34 crystals was grown on the surface of SiC foam. In order to control the growth, loading, and coverage of SAPO-34 crystals on SiC foam surface, different parameters were varied. Namely the effects of the following parameters will be investigated:

### **1.10.1 Effects of Synthesis Duration**

In order to study the crystallization mechanism and crystal growth of SAPO-34 on SiC foams, the morphological evolution was observed as a function of the synthesis time, using scanning electron microscopy (SEM) to identify the morphology, crystal size and coverage after different reaction times.

### **1.10.2 Effects of Number of Coating Cycles**

Fabrication of a continuous layer of SAPO-34 on SiC surface requires repetition of coating cycles; therefore optimization of the number of synthesis times was conducted. The coverage was studied using SEM technique and the loading was quantified by monitoring the increase in the microporous area after each coating step using N<sub>2</sub> adsorption desorption experiment for BET surface area determination, any increase in the microporous area is an indication for the increase in SAPO-34 loading as more SAPO-34 is coated on the foam surface after each synthesis time.

### **1.10.3 Effects of Support Pretreatment**

However, two kinds of support pretreatments was applied and compared in terms of SAPO-34 loading and coverage. Furthermore, the catalytic performance of the two types was evaluated and detailed comparison was conducted.

#### **1. Pretreatments with the template solution**

Pretreatment with the template solution (tetraethyl ammonium hydroxide, TEOH) was performed. The effects of pretreatments were studied using SEM techniques, to compare the coverage and crystal size of the pretreated samples and the non-pretreated SAPO-34/SiC composites.

#### **2. Pretreatments with the precursor solution**

The SiC foam supports were immersed into the zeolite precursor solution for a period of time and heated in an oven in order to dry the SiC foam and form a dense region on the support surface that is reach of nutrients. This kind of pretreatments enhances the growth on the surface rather than in the bulk solution.

## 1.11 Catalytic Testing for Methanol Dehydration to Dimethyl Ether

The as-synthesized SAPO-34/SiC foam composites were tested for the methanol dehydration to dimethyl ether (MTD) in a fixed bed catalytic reactor. Both activity and selectivity of the SAPO-34/SiC foam structured catalyst was evaluated in the MTO reaction, and the catalytic performance was compared for the SAPO-34/SiC composite prepared via slurry coatings and template coatings methods. The methanol conversion and dehydration rates (amount of DME per weight of catalyst) were compared for the two types of composites mentioned earlier at different reaction temperatures.

Moreover, the catalytic performance of the SAPO-34/SiC structured catalyst and SAPO-34 powder was compared in terms of selectivity and DME rate at a temperature of 370 °C and a space velocity of 1000 <sup>-1</sup>h.

## **CHAPTER 4**

### **EXPERIMENTAL SETUP**

#### **1.12 Introduction**

This chapter presents the materials, experimental setup, equipment used in performing all the experiments in this report. Moreover, images of these equipment and instruments will be shown.

The layout of this chapter will be divided into three main parts as similar as the divisions stated earlier in chapter 4 (Research Objectives and plan), and the corresponding experimental methodology will be provided.

### 1.13 SAPO-34 Phase Purity Studies

As stated earlier that a preliminary investigation of SAPO-34 phase purity was conducted in order to select the appropriate concentrations and conditions for pure SAPO-34 using both hydrothermal and microwave assisted synthesis methods.

For the synthesis of SAPO-34 catalyst, a precursor solution was prepared by mixing phosphoric acid (85 wt. %,) with deionized water and tetra ethyl ammonium hydroxide (TEAOH, 25 wt. %) with continuous stirring for 30 min. followed by drop wise addition of colloidal silica (40 wt. % SiO<sub>2</sub> and 0.5 wt.% Na<sub>2</sub>O, Snowtex-40, ST-40). To the above solution, aluminum isopropoxide (98 wt. % Al(OC<sub>3</sub>H<sub>7</sub>)<sub>3</sub>) was added slowly and the solution was further stirred for 2 h. hydrochloric acid (HCl, 37 wt.%) was used to neutralize the pH to about 7. Different formulations used in this study are clearly shown in Table 2.

Regarding the hydrothermal synthesis, the mixture was placed in a stainless steel autoclave PTFE lined (see Figure 17), and heated in an oven at 200 °C for 24 h at static conditions. The solid product was washed with distilled water, dried at 100 °C and subsequently calcined at 550<sup>0</sup> C for 5 h to remove the organic template from the catalyst framework.

In the microwave assisted hydrothermal synthesis method (MAHyS), the precursor solution was transferred in a transparent PTFE autoclave (see Figure 18) and irradiated in a microwave reactor (MicroSYNTH, Milestone, 800 W) as shown in Figure 19. Temperature was raised within 5 minutes to 180 °C.

For the study of the effects of microwave irradiation time, the following molar ratio was used in the synthesis: 0.6 SiO<sub>2</sub> : Al<sub>2</sub>O<sub>3</sub> : P<sub>2</sub>O<sub>5</sub> : 2 TEAOH : 110 H<sub>2</sub>O : 0.7 HCl. the irradiation time was varied starting from 2, 4, and 6 hours.

**Table 1 Different Concentrations for the Synthesis of SAPO-34. Note: HY: Hydrothermal Synthesis, MW: Microwaves Assisted Synthesis.**

Heating Method	Parameter	SiO <sub>2</sub>	Al <sub>2</sub> O <sub>3</sub>	P <sub>2</sub> O <sub>5</sub>	TEAOH	H <sub>2</sub> O	HCl
HY, MW	SiO <sub>2</sub> /Al <sub>2</sub> O <sub>3</sub>	<b>0.1</b>	1.0	1.0	2	110	0.7
		<b>0.3</b>	1.0	1.0	2	110	0.7
		<b>0.5</b>	1.0	1.0	2	110	0.7
		<b>0.7</b>	1.0	1.0	2	110	0.7
HY	TEAOH/Al <sub>2</sub> O <sub>3</sub>	0.6	1.0	1.0	<b>0.5</b>	110	0.7
		0.6	1.0	1.0	<b>1.0</b>	110	0.7
		0.6	1.0	1.0	<b>1.5</b>	110	0.7
		0.6	1.0	1.0	<b>2.0</b>	110	0.7
HY	H <sub>2</sub> O/Al <sub>2</sub> O <sub>3</sub>	0.6	1.0	1.0	2.0	<b>70</b>	0.7
		0.6	1.0	1.0	2.0	<b>90</b>	0.7
		0.6	1.0	1.0	2.0	<b>110</b>	0.7
		0.6	1.0	1.0	2.0	<b>130</b>	0.7



**Figure 17 Stainless Steel Autoclave with PTFE Container**

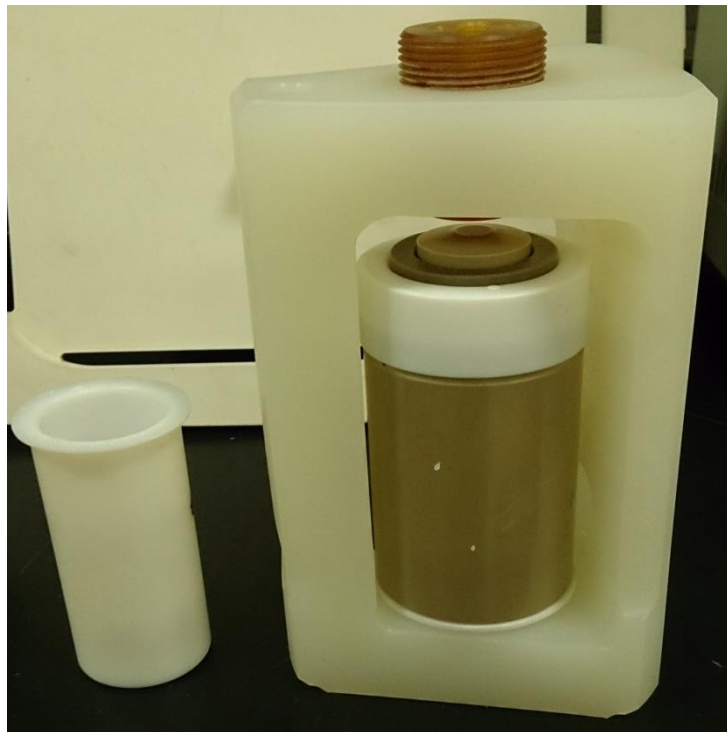


**Figure 18 PTFE autoclave used in MAHyS**

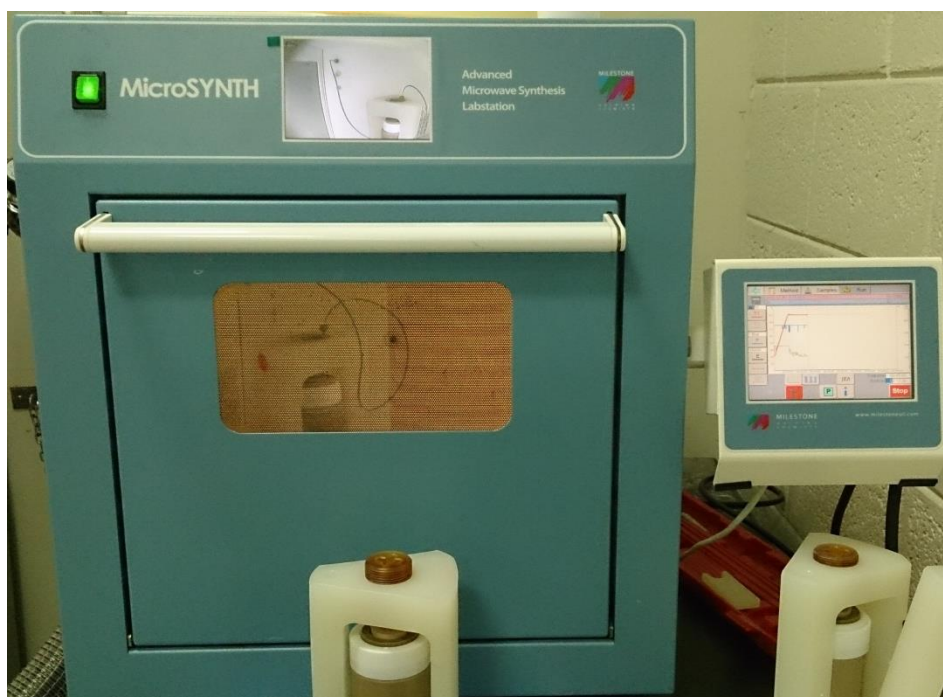


**Figure 19 Microwave Reactor (MicroSynth, Milestone)**

## 1.14 Fabrication of SAPO-34/SiC Foam Composite

An Open cell  $\beta$ -SiC foam (60 PPI), with a BET surface area of  $33 \text{ m}^2/\text{g}$  was obtained from SICAT (France). A Typical size of (1x1x2) cm was placed in a special Teflon holder as shown in Figure 20 and immersed in the precursor solution for SAPO-34 growth (cross section of the reactor is shown in Figure 21). After the reaction, the SiC foams were thoroughly washed with distilled water, sonicated for 10 minutes in a sonication unit to remove the loosely attached crystals and the unreacted solution. The SAPO-34/SiC foam composite dried and calcined under the same conditions as powders. The zeolite loading was determined by hydrofluoric acid HF dissolution of the coated zeolite at room temperature. The loading was calculated on the basis of the total weight of the composite and that of the SiC after the HF treatment.



Figure 20 Specially Designed Teflon Holder

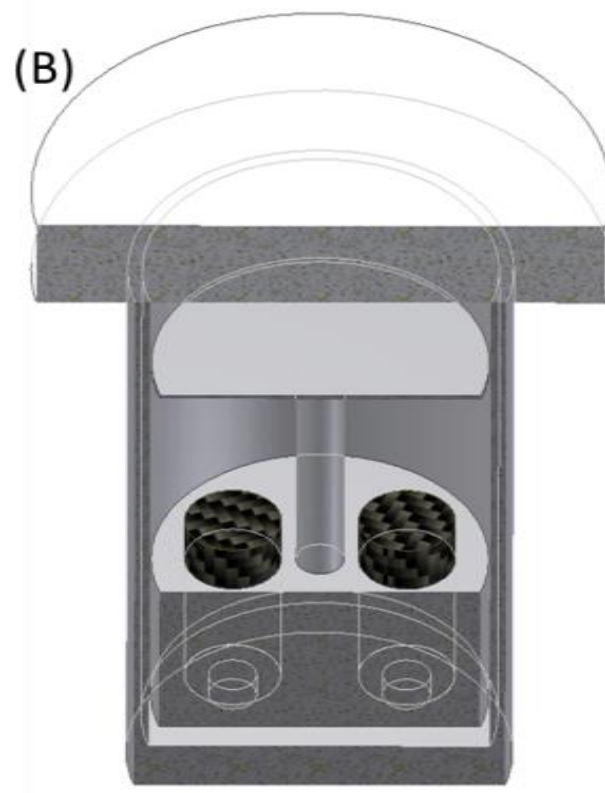


**Figure 21 Cross Section View of the Synthesis Reactor**

## **1.15 Characterization Techniques**

### **1.15.1 X-Ray Diffraction Analysis (XRD)**

Phase identifications and crystallinity were recorded by X-ray diffraction analysis (XRD) on Rigaku RINT D/MAX-2500/PC diffractometer using Cu-K $\alpha$  radiation ( $\lambda = 1.5418 \text{ \AA}$ ) with 30 kV and 15 mA. XRD were run on both the co-precipitated powder and SiC foam samples.

### **1.15.2 Scanning Electron Microscopy (SEM)**

Morphology and crystal's coverage on SiC substrate were investigated by field-emission scanning electron microscopy (FE-SEM, LYRA 3 Dual Beam, Tescan) operated at 30kV acceleration voltage. Samples were coated with gold prior to FE-SEM measurements.

### **1.15.3 Nitrogen Adsorption-Desorption Experiment for BET surface Area**

The Brunatuer-Emmett-Teller (BET) surface area, of the composite catalyst was determined by N<sub>2</sub> adsorption-desorption measurements at 77 K (Micromeritics sorptomoeter Tri Star 3000). Prior to N<sub>2</sub> adsorption, the samples were degassed at 573 °C for 4 h in order to desorb water and moisture from the surface and inside the porous network.

## 1.16 Methanol Dehydration to Dimethyl Ether (MTD)

The methanol dehydration to dimethyl ether (DME) was carried out in an all glass microreactor. The catalyst was deposited on a quartz wool plug inside a tubular reactor (ID 12 mm, length, 400 mm) housed inside an electrical oven equipped with two thermocouples, one inside the oven and one next to the reactor wall. Methanol was supplied by bubbling an argon flow through a methanol saturator kept at 30 °C leading to a methanol concentration of 21 vol. % in the reactant mixture. The total gaseous space velocity (GHSV) was fixed at 4500 h<sup>-1</sup> corresponding to a total CH<sub>3</sub>OH/Ar flow rate of 80 mL/min. The reactant and products were analyzed on line with a gas chromatography (GC) equipped with a Flame Ionisation Detector (FID) and CP-Sil5 column allowing the detection of hydrocarbons from C<sub>1</sub> to C<sub>10</sub>. The dehydration reaction was carried out at different temperatures ranging from 350 °C to 400 °C at atmospheric pressure.

$$GHSV = \frac{\dot{m}_{Meth.@STP}}{m_{Catalyst}}$$

In other words, GHSV is the ratio of methanol gaseous flow rate at STP conditions to the mass of SAPO-34 catalyst.

The methanol conversion was calculated from the difference between the methanol concentration in the inlet and outlet of the reactor.

$$X_{Meth.} = \frac{C_{Meth,in} - C_{Meth,out}}{C_{Meth,in}}$$

The DME selectivity was defined as the molar ratio of the hydrocarbon produced versus methanol converted.

$$Selectivity = \frac{n_{DME,out}}{n_{Meth,in} - n_{Meth,out}}$$

The amount of carbonaceous residus deposited on the catalyst surface was also investigated by means of the temperature-programmed oxidation (TPO). The sample was packed inside a vertical quartz reactor housed inside an electric furnace. The sample was flushed with helium flow (50 mL/min) at room temperature (RT) for 30 minutes and then the helium flow was replaced by a mixture of O<sub>2</sub> (20 vol. %) diluted in helium with a flow rate of 50 mL/min. The reactor temperature was raised from RT to 800 °C (heating rate of 10 °C/min). The CO<sub>2</sub> and CO formed were monitored with a mass spectrometer and thermal conductivity catharometer (TCD).

## CHAPTER 5

### RESULTS AND DISCUSSION

#### 1.17 Introduction

In this chapter the results obtained in this study were introduced, and scientific discussion of the results was presented along with comparisons of the results with previous literature. Also the impact and the importance of this work have been thoroughly discussed.

Again, the results were divided into three major parts, and the corresponding discussions were conducted on each part.

Results of preliminary studies on SAPO-34 phase purity were shown at the beginning of this chapter, followed by the optimization of the parameters in the growth of the SAPO-34 crystals on the surface of the SiC foam support and showing all the characterizations been performed. Finally, the catalytic performance of both the SAPO-34/SiC foam structured catalyst and the SAPO-34 powder were compared, showing the effects of different reaction conditions on the activity, selectivity and the stability of the catalysts in the methanol dehydration to dimethyl ether.

## 1.18 Results of SAPO-34 Phase Purity Studies

### 1.18.1 Hydrothermal Synthesis Method

#### 1. Effects of Si/Al ratio

Influence of different reagents concentrations was studied and their effects on phase purity were demonstrated. Figure 22 shows the effect of Si/Al ratios on the resulting XRD patterns. At low Si/Al ratios ( $\text{SiO}_2/\text{Al}_2\text{O}_3 = 0.1$  and  $0.3$ ), the presence of crystalline phase of SAPO-18 as impurity was confirmed, which was completely disappeared by increasing the Si/Al ratio ( $\text{SiO}_2/\text{Al}_2\text{O}_3 = 0.5$ ), resulting in a formation of pure SAPO-34 with a characteristic peaks similar to the reported SAPO-34 patterns in reference [65]. Further increasing the Si/Al ratio ( $\text{SiO}_2/\text{Al}_2\text{O}_3 = 0.7$ ) resulted in an improvement of the crystallinity as can be seen from the increase in the peak intensities, with no impurities observed. Formation of SAPO-18 at low Si/Al ratios as a competing phase with the dominant SAPO-34 is discussed by A. Izadbakhsh et al [7] and it was attributed to the silicon source used (colloidal silica) which has particle size that favors easier incorporation of Si to SAPO-18 framework at low silicon concentrations.

#### 2. Effects of Template Concentration

The use of organic templates as structure directing agents is vital for the synthesis of zeolite materials [66]. Varying the concentration of the template material in the solution affected both crystallinity and purity of the samples. Figure 23 shows the XRD patterns of samples obtained at different TEAOH concentrations. At very low concentrations i.e  $\text{TEAOH}/\text{Al}_2\text{O}_3 = 0.5$  a dense phase of aluminum phosphate was formed, which indicates that Si did not incorporate into the framework. However, the concentration of

TEAOH/Al<sub>2</sub>O<sub>3</sub> = 1.0 resulted in pure SAPO-5 phase. SAPO-34 was obtained at TEAOH/Al<sub>2</sub>O<sub>3</sub> = 1.5, with the presence of SAPO-18 as impurity, whereas pure SAPO-34 was only obtained at TEAOH/Al<sub>2</sub>O<sub>3</sub> = 2.0. The observations above proved that the template molar ratio is crucial to the synthesis of pure SAPO-34. Moreover, the low template concentrations favored the formation of SAPO-5 while SAPO-34 can only produce at relatively high template ratios.

### 3. Effects of water concentration

All the syntheses with different dilution ratios produced pure crystalline SAPO-34 molecular sieve, with H<sub>2</sub>O/Al<sub>2</sub>O<sub>3</sub> ratio of 110 exhibited the higher crystallinity, as can be deduced from Figure 24.

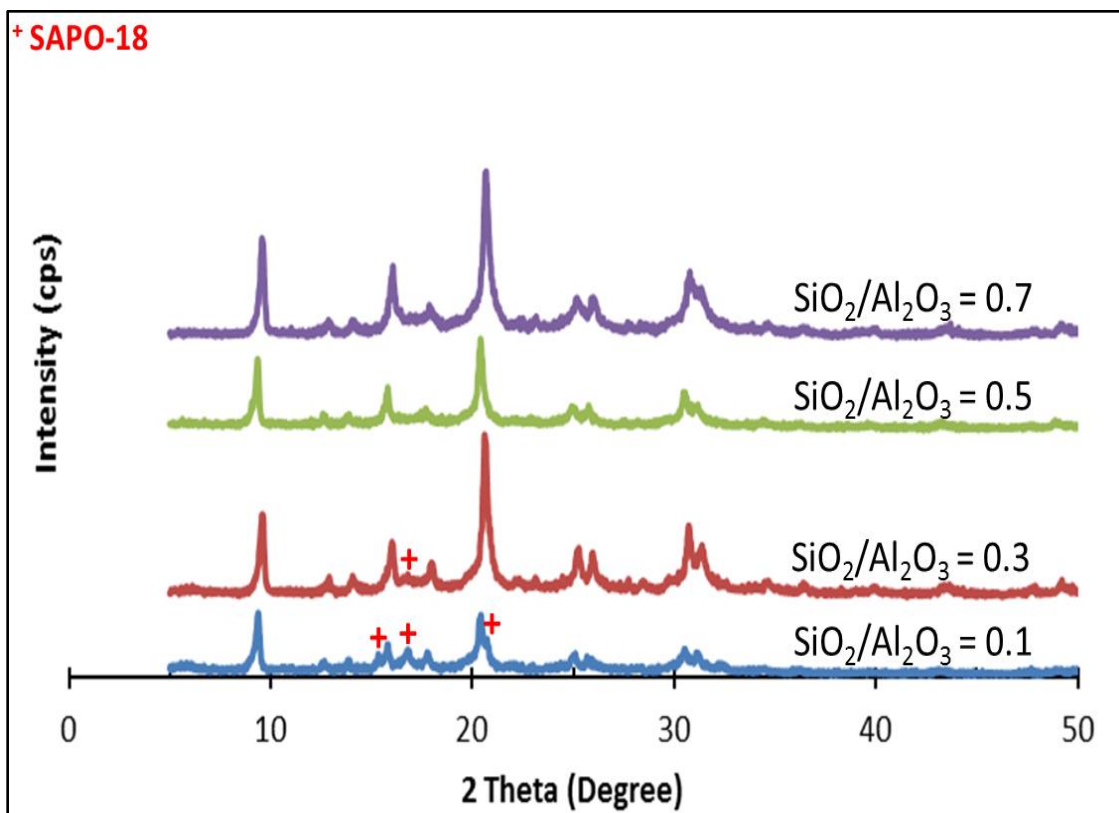


Figure 22 XRD Patterns of As-synthesized Samples Using Hydrothermal Synthesis (200 °C, 24 h): Effects of SiO<sub>2</sub>/Al<sub>2</sub>O<sub>3</sub>

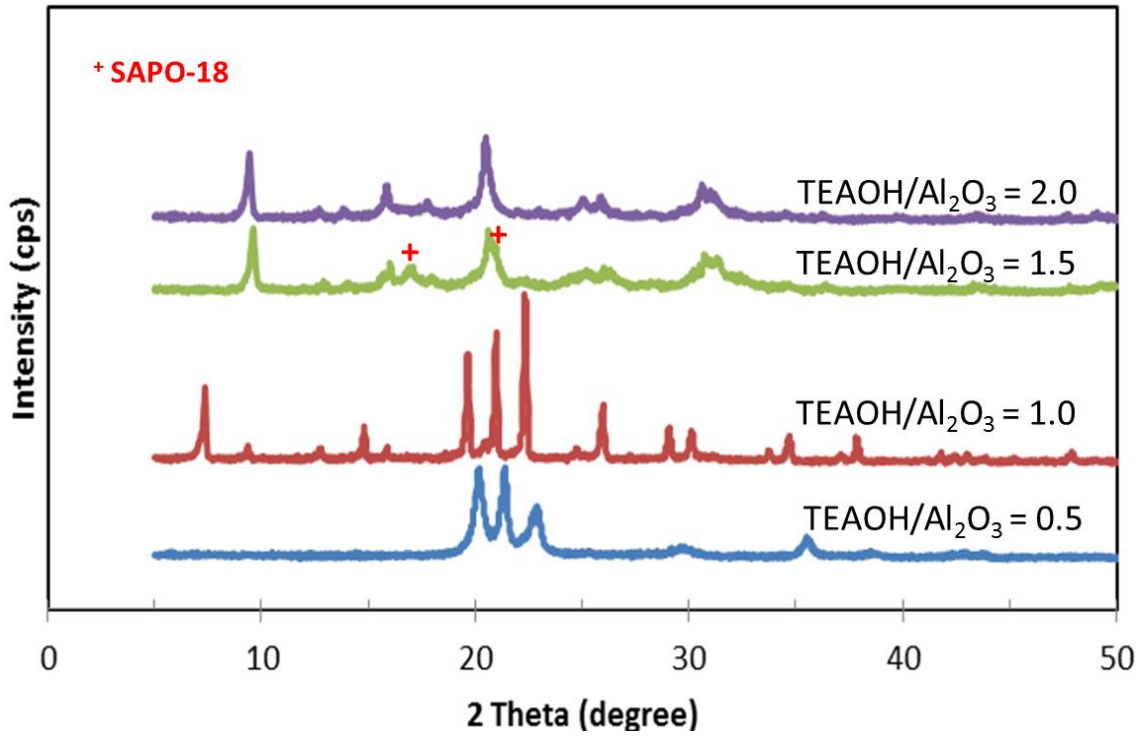


Figure 23 XRD Patterns of Samples Using Hydrothermal Synthesis (200 °C , 24 h): Effect of TEAOH Concentration

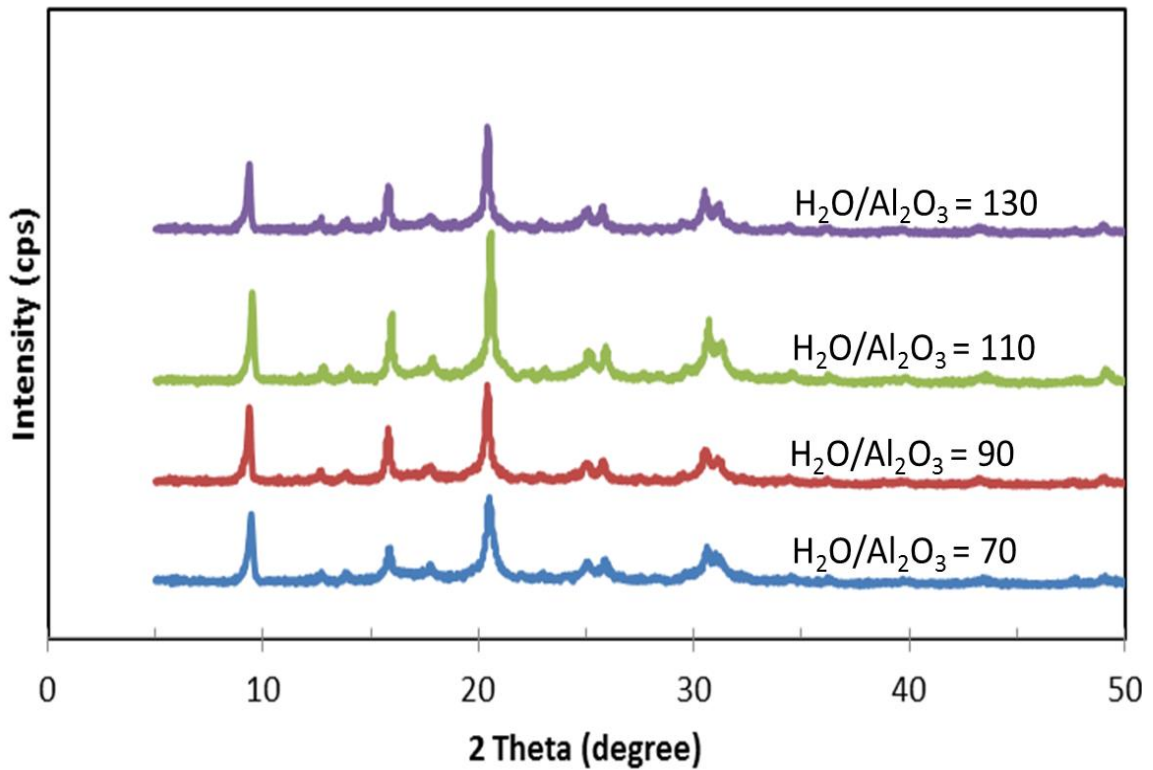


Figure 24 XRD Patterns of Samples Using Hydrothermal Synthesis (200 oC, 24 h): Effect of Water Concentration

### 1.18.2 Microwave Assisted Hydrothermal Synthesis Method (MAHyS)

Microwave mediated synthesis of zeolites has gained considerable attention, providing enhanced crystallization time and reduced crystal size. In this work, microwave irradiation has been applied for the preparation of SAPO-34 and different Si/Al ratios of the starting gel were employed. Figure 25 shows the XRD patterns of the prepared samples. At low Si/Al ratio ( $\text{SiO}_2/\text{Al}_2\text{O}_3 = 0.2$ ), SAPO-18 and  $\text{AlPO}_4$ -Tridymite co-crystallized with SAPO-34 at the given reaction conditions, whereas pure SAPO-34 was obtained at all formulations with higher Si/Al ratios. The most significant advantage of using microwave assisted method is the remarkable decrease of reaction time (6 h) as compared to the conventional heating method (24 h).

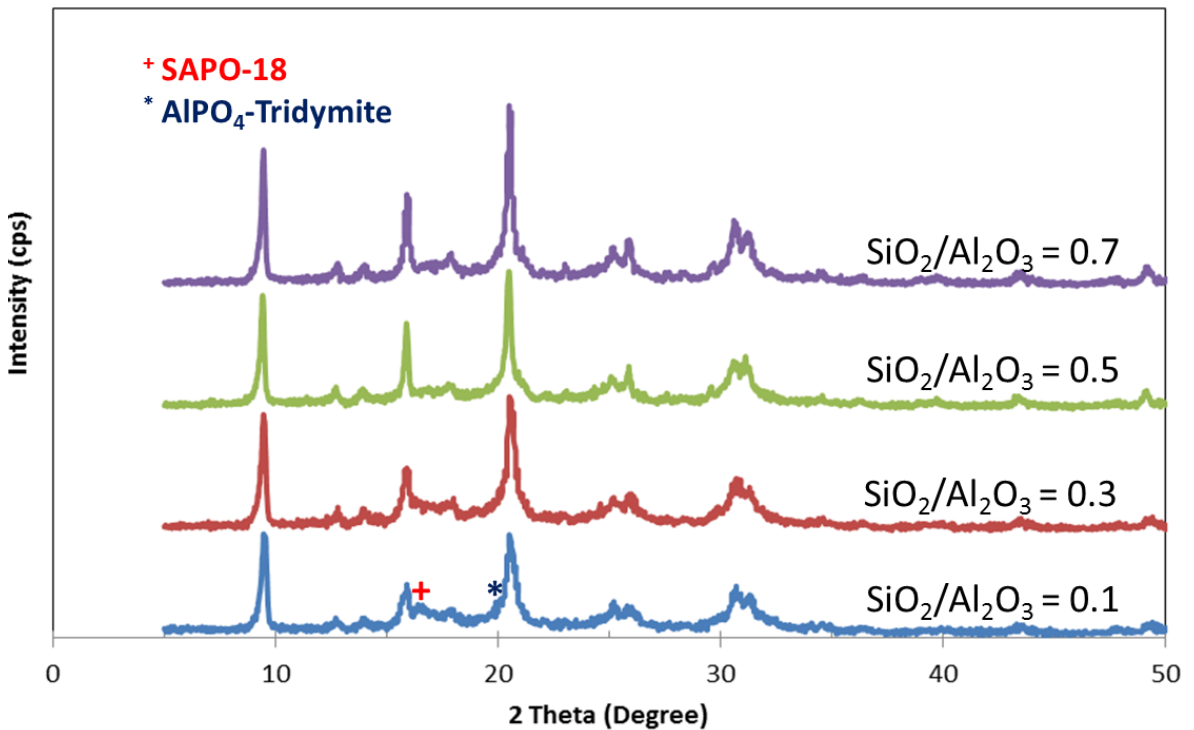
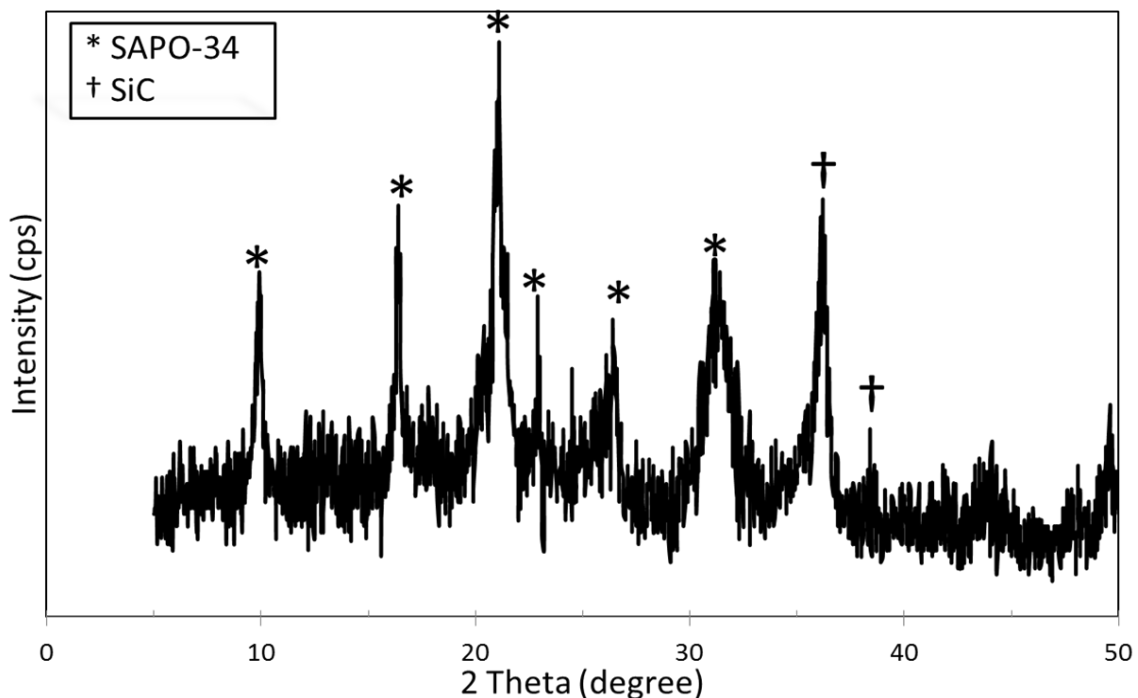


Figure 25 XRD Patterns of As-synthesized Samples Using Microwave Irradiation (180 °C, 6 h): Effects of  $\text{SiO}_2/\text{Al}_2\text{O}_3$

## **1.19 Fabrication and Characterization of SAPO-34/SiC Foam Composite**

### **1.19.1 Fabrication of the SAPO-34/SiC Foam Structured Catalyst**

All the attempts to grow SAPO-34 on SiC foam via conventional heating method were failed due to the attachment of the co-precipitated powders on the foam surface at the reaction conditions (200 °C and 24 h), which could not be removed even after thorough washing and sonication cycles. On the other hand, microwave mediated synthesis produced samples free of any hanging extra-particles because of the short reaction time (6 h). The X-ray diffraction pattern (XRD) of the SAPO-34/SiC foam composite is shown in Figure 26. Strong diffraction peaks of the CHA structure (SAPO-34 phase) was recorded, together with peaks corresponding to the SiC support, which has relatively lower intensities, indicating the formation of thick SAPO-34 coatings on the SiC foam substrate.



**Figure 26 XRD Pattern of SAPO-34/SiC Foam Composite, Synthesized at 180 °C for 6 h Microwave Irradiation**

SEM photographs of the SAPO-34/SiC foam structure after 4 coating cycles are presented in Figure 27. The opened cell structure of the SiC foam, made of struts, cells and windows is clearly shown in Figure 27a. Full coverage of the SiC struts was observed (Figure 27b), without blocking of the pores with the SAPO-34 crystals. Figure 27c is a magnified view of the SiC foam surface showing the microstructure and morphology of the zeolite layer grown on the surface of the SiC foam and it is clearly observed that the macropores in the SiC foam were fully covered with the SAPO-34 crystals indicating that the solution effectively penetrates into the SiC pores during the microwave irradiation. It was also observed that the SAPO-34 coatings constituted in a form of interconnected cubic crystals (Figure 27d) rather than forming distinct layers, confirming the findings of Bonaccorsi and co-workers [67]. This could be attributed to the secondary growth of the previously formed crystals after the repetition of coating times which occurred

simultaneously with the formation of new crystals. The corresponding specific surface area of the SAPO-34/SiC composite after the four coating cycle was reported to be 80 m<sup>2</sup>/g. The low surface area measured could be attributed to the intergrowth of the zeolite within the seeding layer which leads to the formation of a dense zeolite layer with low porosity and accessibility (see Figure 38).

According to the BET results one can stated that slurry coating seems not to be a viable synthesis route as it is strongly decrease the specific surface area of the catalyst even after the four coating cycles. Especially when it is taken into account the relatively high specific surface area of the bulk SAPO-34 zeolite reported in the literature [7]. The catalyst after four coating cycle will be further evaluated in the methanol dehydration into dimethylether.

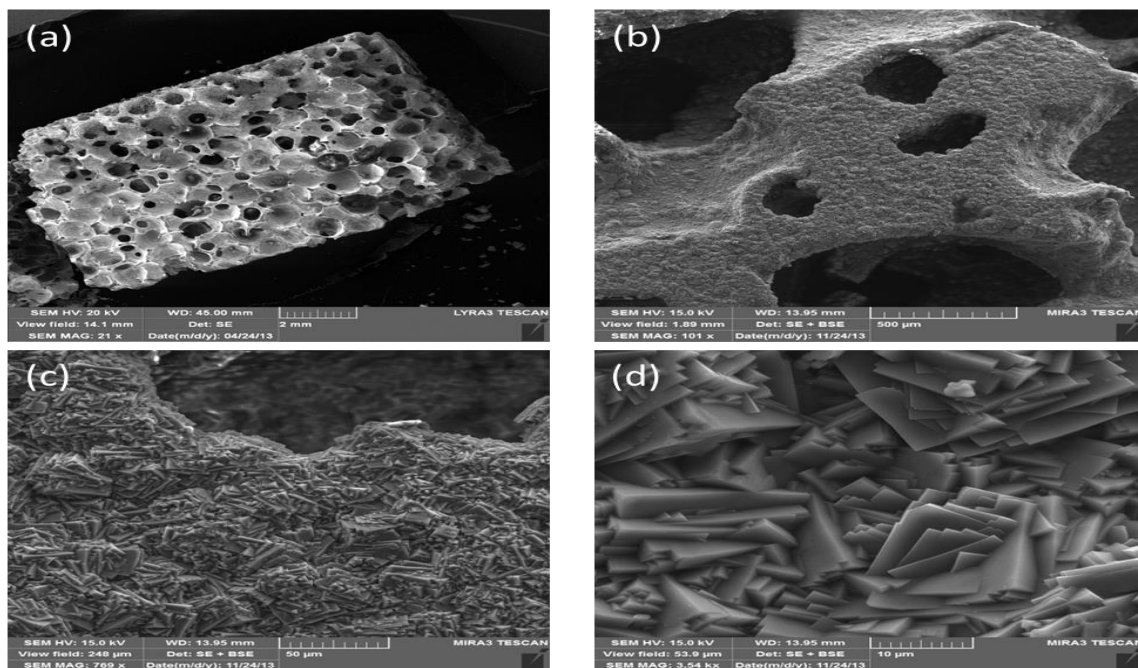


**Figure 27 SEM images of (a) the SiC foam, (b) Struts of the SiC foam, (c) Struts Covered with a Continuous Layer of SAPO-34 Catalyst and (d) Magnified View of SAPO-34 Crystals**

### 1.19.2 Effects of Microwave Irradiation Time

The evolution of the zeolite crystals on the surface of SiC foams was studied at different microwave irradiation times. A precursor solution with a molar ratios of 0.6 SiO<sub>2</sub> : 1.0 Al<sub>2</sub>O<sub>3</sub> : 1.0 P<sub>2</sub>O<sub>5</sub> : 2.0 TEAOH : 110 H<sub>2</sub>O : 0.7 HCl, was used in these experiments.

After substrate pretreatment with the precursor solution, the SiC foam surface was fully covered with a dense gel film (Figure 28a), this supersaturated region on the substrate surface enhanced the rapid nucleation on the support, and consequently the heterogeneous crystallization during the microwave irradiation process. Furthermore it favored the direct growth on the support, which strengthened the attachment of the crystals to the SiC surface and thus increased the life time of the composite catalyst. The importance of solution pre-adsorption in the synthesis of the ZSM-5 zeolite membrane was reported by Li and co-workers [68]. After 2 h microwave irradiation (Figure 28b) some crystals possessing incomplete-cubic morphology, started to bond to the surface with sizes of about 7 μm. Further increasing the reaction time to 4 h (Figure 28c) did not show any noticeable increase in crystal size, but improved the homogeneity of crystal growth. Sharp cubic morphologies were obtained at 6 h irradiation time (Figure 28d) with the same average crystal size (7 μm).

Jiao and co-workers [36] has studied the effect of synthesis time on the in-situ growth of ZSM-5 on SiC foams using conventional ovens, where they reported the increase of crystal size with increasing the time up to 36 h. However in this study the observations implied that, the increase in microwave irradiation time did not affect the crystal size of the coated zeolite, but improved the crystallinity of SAPO-34 zeolite. This could be

further confirmed by the increase in the intensities of the XRD patterns of the SAPO-34 powders collected from the bottom of the microwave unit (Figure 29).

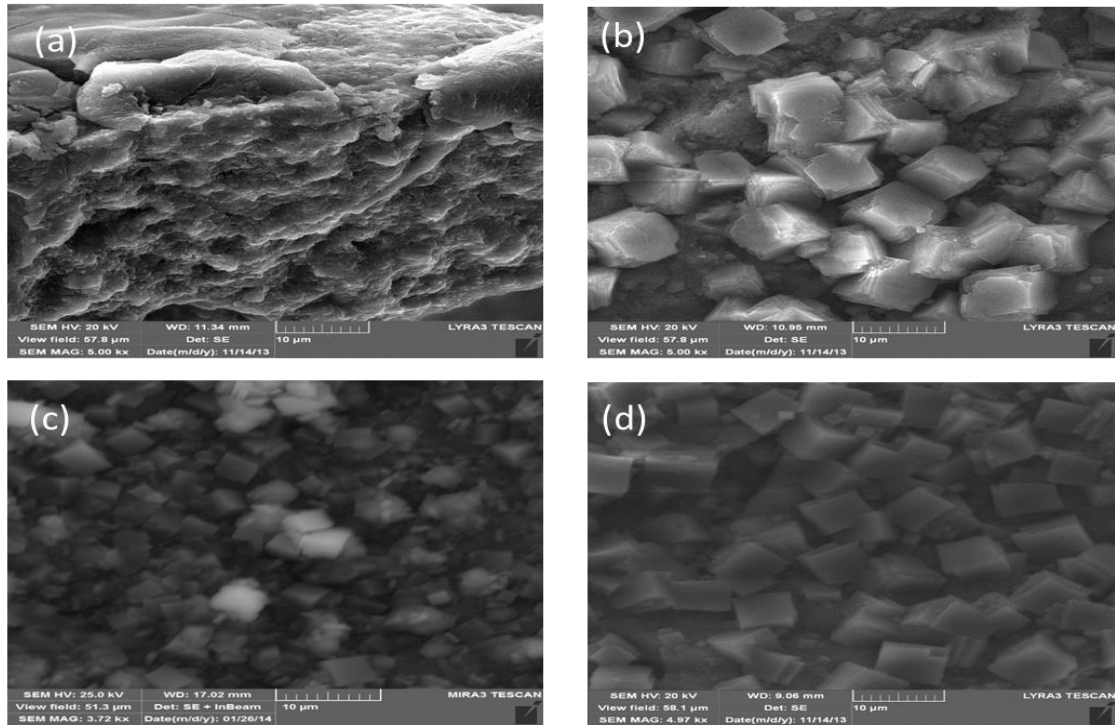


**Figure 28 SEM Images of (a) SiC Foam Modified with the Precursor Solution, (b-d) SAPO-34/SiC Foam Composite After 2, 4, and 6 h Microwave Irradiation**

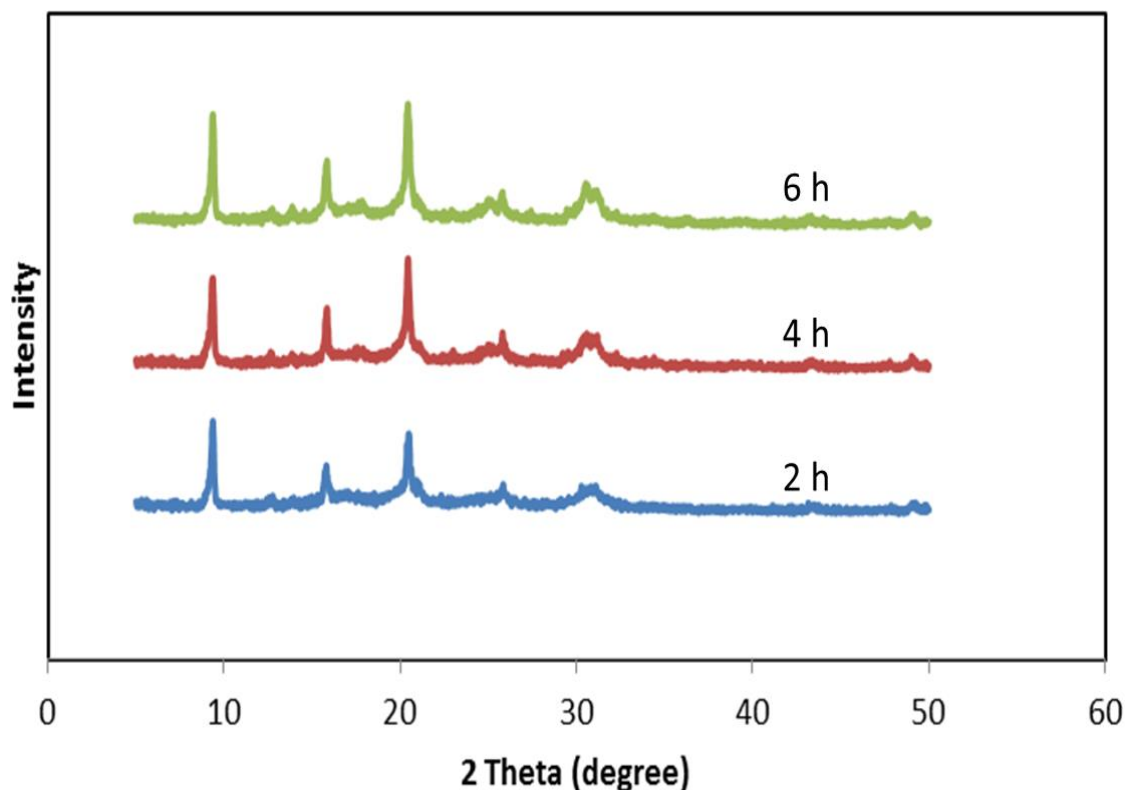


Figure 29 XRD Patterns of SAPO-34 Samples at Different Microwave Irradiation Times

### 1.19.3 Effects of Number of Coating Cycles

The loading of SAPO-34 crystals has potential impacts on the performance of the composite catalyst [16]; therefore the number of synthesis steps which significantly affect the loading amount was investigated.

The BET surface area after each synthesis step as a function of the number of synthesis cycles is presented in Figure 30. It can be clearly observed that the specific surface area of the SAPO-34/SiC foam composite markedly increased with the repetition of coating cycles, indicating that more deposition of SAPO-34 layers was achieved after each synthesis time. It can also be deduced that after the first coating cycle the loading of SAPO-34 crystals was very low (see Figure 31) which increased by about seven times

after the second coating step. Moreover, the increase in BET surface area was also noticeable after the thied coating cycle. However, slight decrease was recorded after the 4<sup>th</sup> synthesis time as compared to the previous cycles which could be attributed to the increase in crystal size of the previously formed crystals instead of forming new SAPO-34 layers.

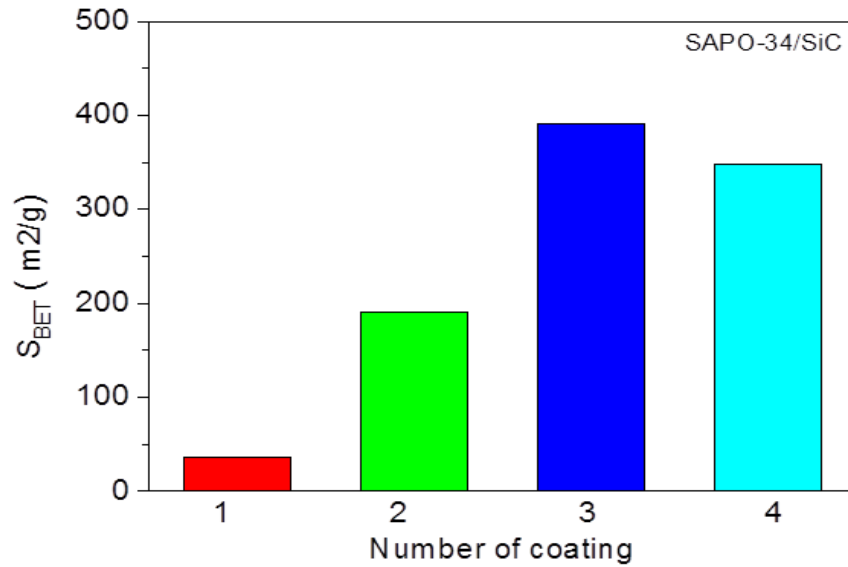


Figure 30 BET Surface Area versus Number of Coating Cycles

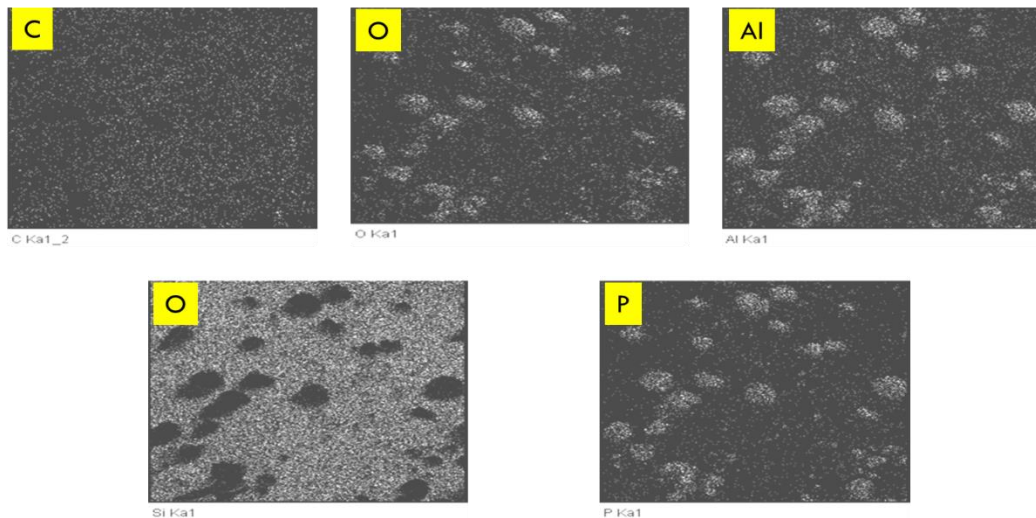


Figure 31 EDX Compositional Mapping After the 1<sup>st</sup> Coating Cycle

Figures 32 to 35 shows the textural properties of the SAPO-34/SiC foam composites after different synthesis times, and Figure 36 shows the N<sub>2</sub> adsorption-desorption isotherm of the SAPO-34 powder prepared at the same conditions and collected from the bottom of the Teflon.

The SAPO-34 powder has shown total BET surface area of about 460 m<sup>2</sup>, which is greater than the SAPO-34/SiC foam composite after the 4<sup>th</sup> coating step.

Gu et al in 2010 [47] have studied the effect of the number of coating cycles using N<sub>2</sub> adsorption-desorption experiment and BET method, and they obtained similar trends where BET surface area increased with the repetition of the synthesis process.

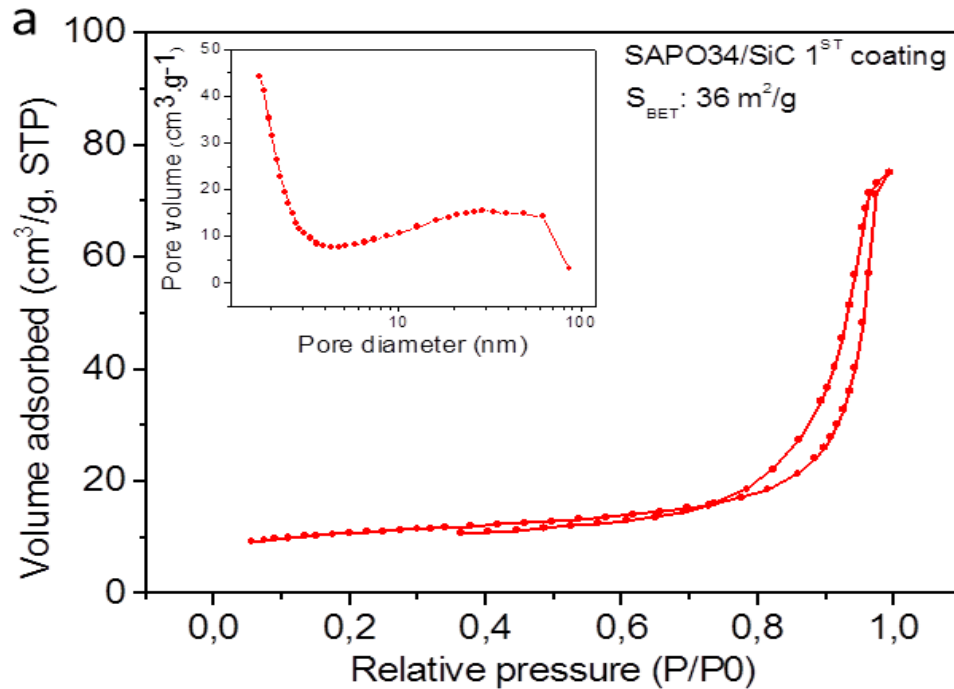


Figure 32 N<sub>2</sub> Adsorption-desorption Experiment After the 1<sup>st</sup> Coating Cycle

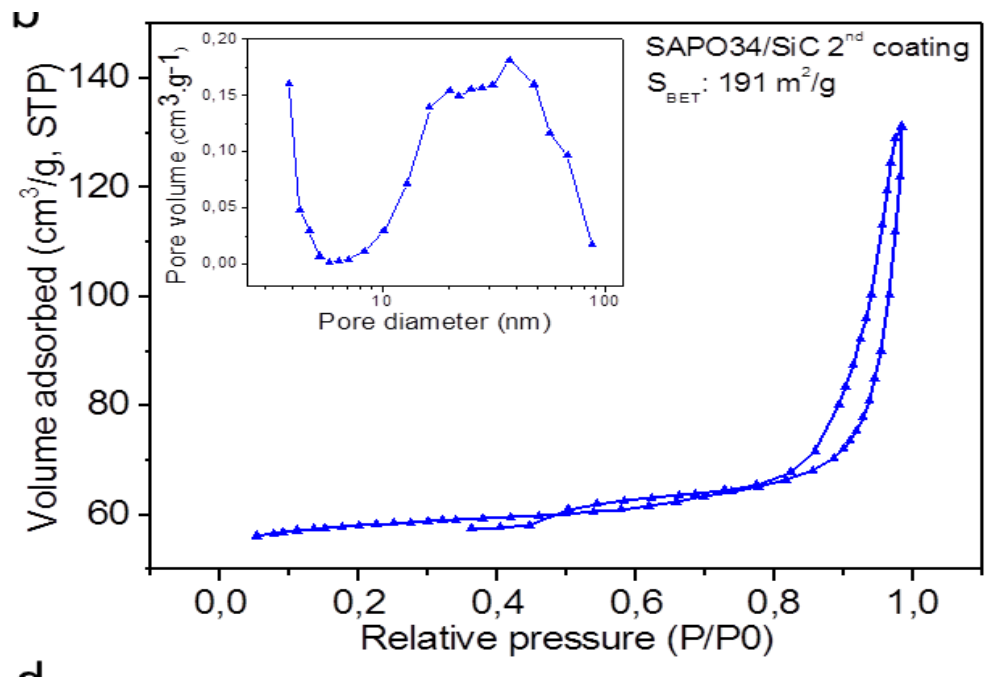


Figure 33 N<sub>2</sub> Adsorption-desorption Experiment After the 2<sup>nd</sup> Coating Cycle

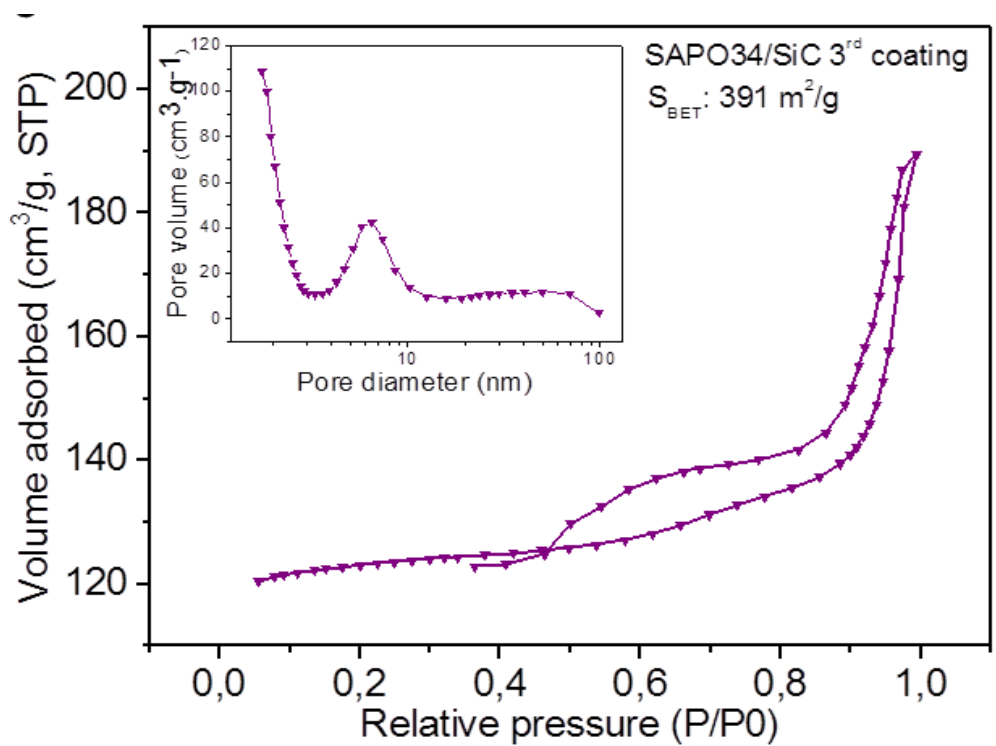


Figure 34 N<sub>2</sub> Adsorption-desorption Experiment After the 3<sup>rd</sup> Coating Cycle

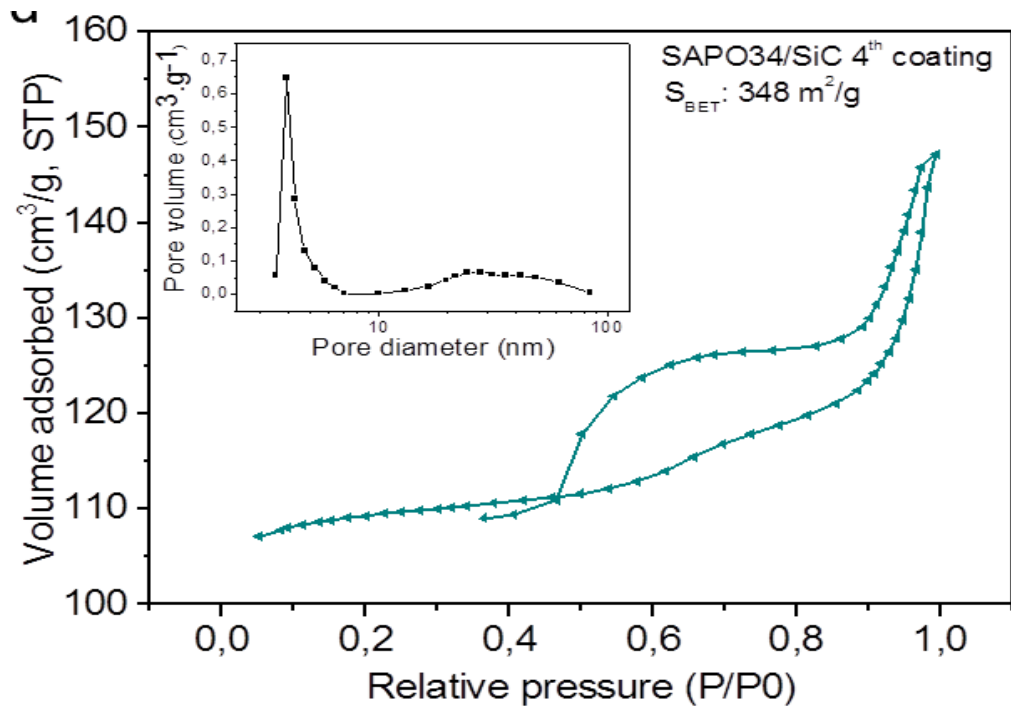


Figure 35 N<sub>2</sub> Adsorption-desorption Experiment After the 4<sup>th</sup> Coating Cycle

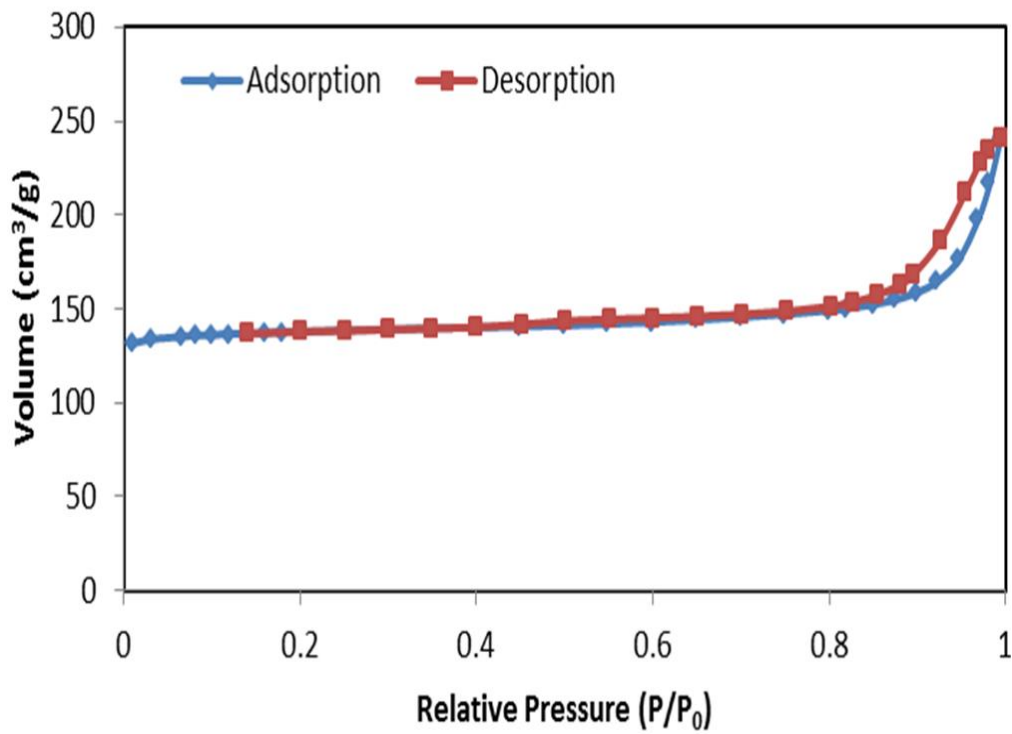


Figure 36 N<sub>2</sub> Adsorption-desorption Experiment for SAPO-34 Powder Using MAHyS (180 °C, 6 h)

#### 1.19.4 Effects of Pretreatment with the Template Material (TEAOH)

The effect of template pretreatments of the SiC support is demonstrated in Figure 37. The surface of the bare SiC foam surface is shown in Figure 37a. Pretreatments with the template material resulted in the formation of a smooth layer of TEAOH solution as shown in Figure 37b. In situ growth on the non-pretreated foams resulted in an incomplete coverage of SAPO-34 crystals having an average size of 7  $\mu\text{m}$  as shown in Figure 37c. However, it is clearly observed that, significant enhancement of coverage was obtained with the pretreated samples (Figure 37d). The positive effect of pretreating support materials with template solutions was reported by Van Der Puil et al. [69]. The layer of the template solution formed on the support surface after pretreatment was responsible for the surface activation which caused considerable induction of the heterogeneous nucleation. Moreover, it strengthened the bonds between the crystals and the support surface. The zeolite loading determined by selective HF dissolution was amounted to about 53 wt. % after third cycles coating with specific surface area of about 400  $\text{m}^2/\text{g}$  as compared to 80  $\text{m}^2/\text{g}$  for the slurry pretreatment route.

The high specific surface area of the samples synthesized through a template coating method compared to that obtained on the samples prepared through the zeolite precursor coating could be explained by the smaller average zeolite crystal size in the case of the template coated sample. Indeed, the zeolite size in the template coating (Figure 37d) is slightly smaller than that of the one synthesized through the slurry coating (Figure 27d). The template coating could also leads to the formation of a zeolite layer with higher porosity and thus, higher accessible surface area, compared to the zeolite coating route. The pore size distribution between the two tested catalysts is presented in Figure 38 and

clearly evidences the higher porosity in the sample synthesized through template coating than the one with the slurry coating.

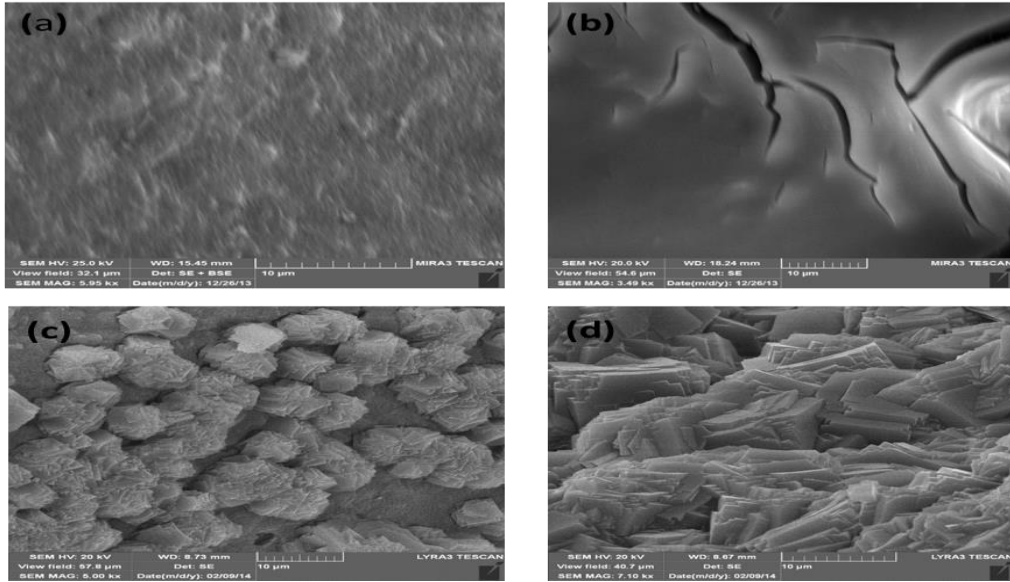


Figure 37 Effect of Template Pretreatments of SiC foam, (a) Surface of Bare SiC foam, (b) Support Pretreated with TEOH Solution for 1 h, (c) After 2<sup>nd</sup> Coating Step without Template Pretreatments, (d) After 2<sup>nd</sup> Coating Step with Template Pretreatment

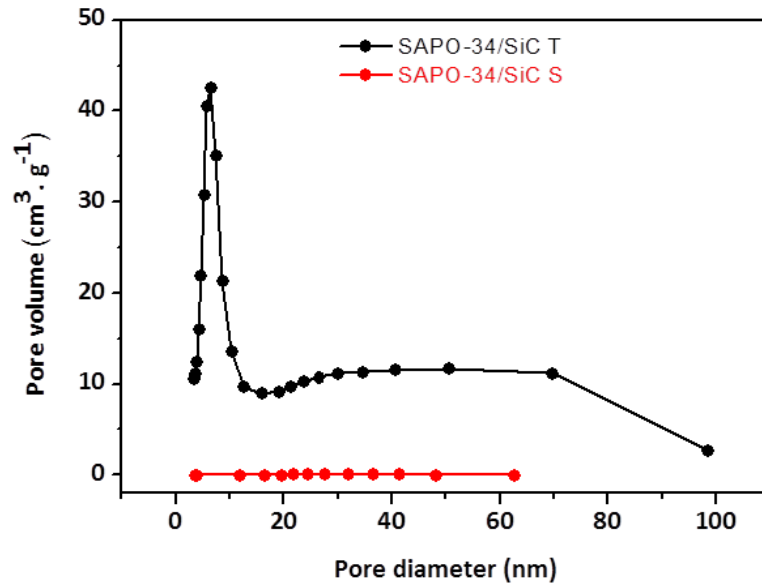


Figure 38 Pore Size Distribution Determined from the Desorption Branch of the Nitrogen Isotherm on the SAPO-34/SiC Synthesized via Template (Black) and Slurry (Red) Coating

## **1.20 Methanol Dehydration to Dimethyl Ether (MTD)**

The methanol dehydration into DME on the SAPO-based catalysts deposited on SiC foam, synthesized either by slurry coating and template seeding, as a function of time on stream is presented in Figure 39 and 40 respectively at different temperatures and fixed space velocity. The supported SAPO-34/SiC foam catalysts tested were the one obtained after the fourth slurry coating cycles and the third template seeding cycles in order to ensure the complete coverage of the SiC foam surface by an homogeneous layer of SAPO-34. The two catalysts are also being selected owing to their high specific surface area according to the BET measurements. The weight of the catalyst was selected according to the hydrofluoric dissolution experiment (HF treatment) in order to have a similar zeolite weight in the reactor. The catalytic dehydration results obtained on these catalysts are presented in Figure 39 and 40 as a function of the reaction conditions. The comparison is made on the basis of the methanol conversion and specific dehydration activity ( $\text{mol}_{\text{DME}}/\text{g}_{\text{SAPO34}}/\text{h}$ ) on the two catalysts. The zeolite loading was determined by HF treatment at room temperature.

### **1.20.1 Comparison of the Dehydration Activities of Slurry and Template Seeded SAPO-34/SiC Foam Composites**

According to the results the dehydration specific rate was different between the two tested catalysts at a relatively high space velocity of  $4500 \text{ h}^{-1}$  (STP). The dehydration activity obtained on the template coated catalyst, SAPO-34/SiC-T, is higher than the one obtained on the slurry coated catalyst, SAPO-34/SiC-S, especially at low reaction temperature ( $350 \text{ }^{\circ}\text{C}$ ). It is worthy to note that the difference in terms of DH activity

becomes less pronounced on both catalysts at higher reaction temperature. The DME selectivity is similar on both the tested catalysts at around 95 % at 350 °C and 90 % at 400 °C.

The high dehydration activity of the template catalyst at low reaction temperature could be attributed to the high specific surface area which exhibit higher active site density for performing the reaction. Such advantage is reduced when the reaction is carried out at higher temperature as the activity per active site also strongly increases with increasing the reaction temperature. It is also worthy to note that at high reaction temperature the methanol conversion becomes close to the thermodynamic equilibrium (80 %), and thus, the difference in terms of the dehydration activity is less pronounced. According to the catalytic results one can stated that the template seeding route is more appropriate for preparing SiC supported SAPO-34 catalyst than the slurry pre-impregnation method. It is also worthy to note that the Si incorporation into SAPO-34 framework could be different in the slurry and the template pretreated samples. Additional work should be carried out to investigate the acidity and Si/Al ratio between the two catalysts in order to clarify this point.

It is also worthy to note that the methanol dehydration on both catalysts is extremely stable as a function of time on stream which indicates that deactivation through pore plugging is unlikely to occur. Such high stability has already been reported in the case of supported H-ZSM-5 zeolite by Ivanova et al. [16] and was attributed to the high escaping rate of the intermediate product through the zeolite layer which significantly reduced the catalyst plugging by carbonaceous formation within the pore size of the zeolite.

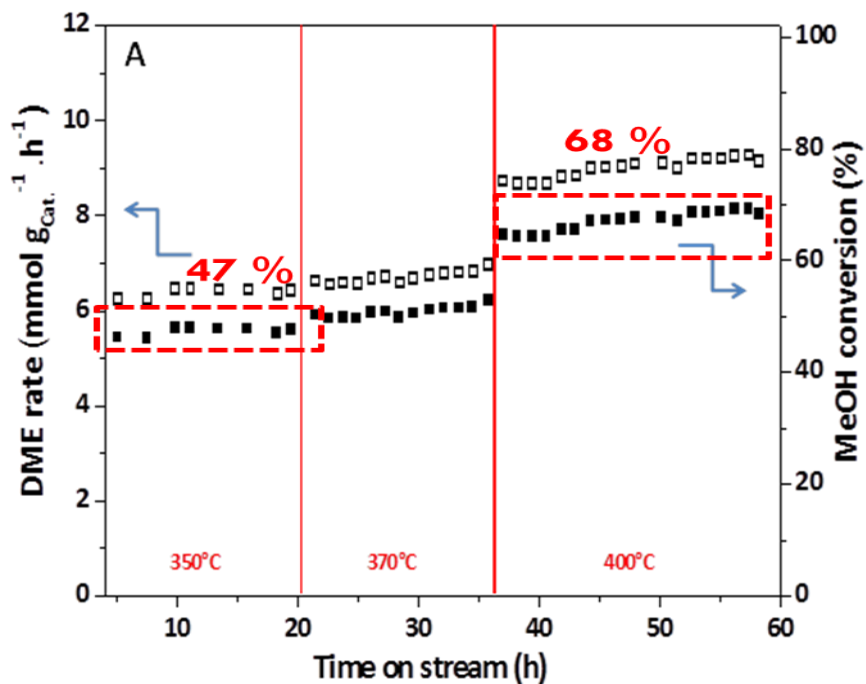


Figure 39 Methanol Conversion and Specific Dehydration Rate of the Methanol on the SAPO-34 Catalysts Synthesized by Slurry Coating (SAPO-34/SiC-S), Reaction Conditions: Atmospheric Pressure, GHSV = 4500 h<sup>-1</sup>, Catalyst Weight = 0.8 g, SAPO-34 Weight = 0.45

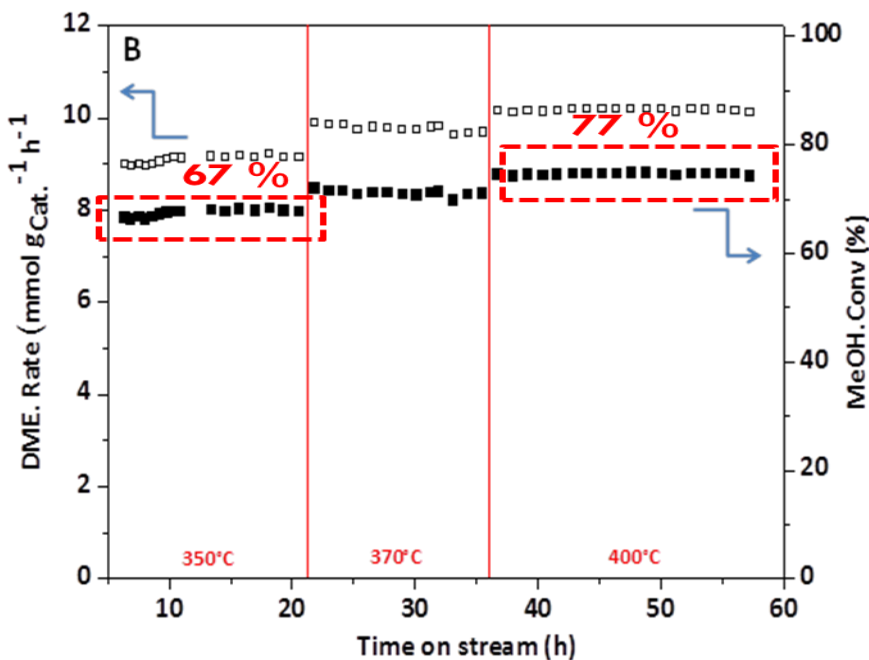


Figure 40 Methanol Conversion and Specific Dehydration Rate of the Methanol on the SAPO-34 Catalysts Synthesized by Template Coating (SAPO-34/SiC-T), Reaction Conditions: Atmospheric Pressure, GHSV = 4500 h<sup>-1</sup>, Catalyst Weight = 0.8 g, SAPO-34 Weight = 0.45

Figure 41 and 42 show the effect of reaction temperature on methanol conversion for SAPO-34/SiC-S and SAPO-34/SiC-T composites respectively.

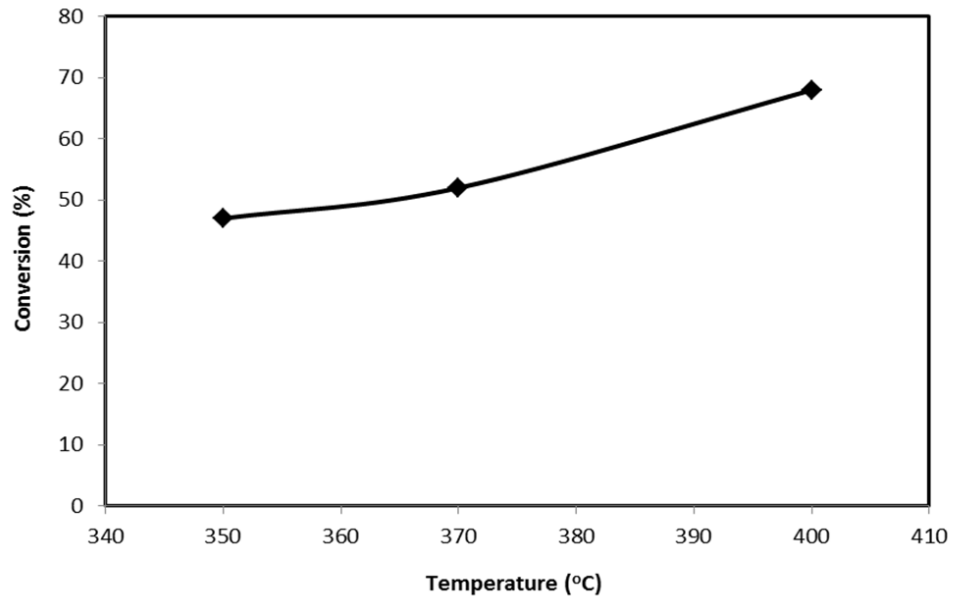


Figure 41 Conversion vs Temperature for Template coating (SAPO-34/SiC-S)

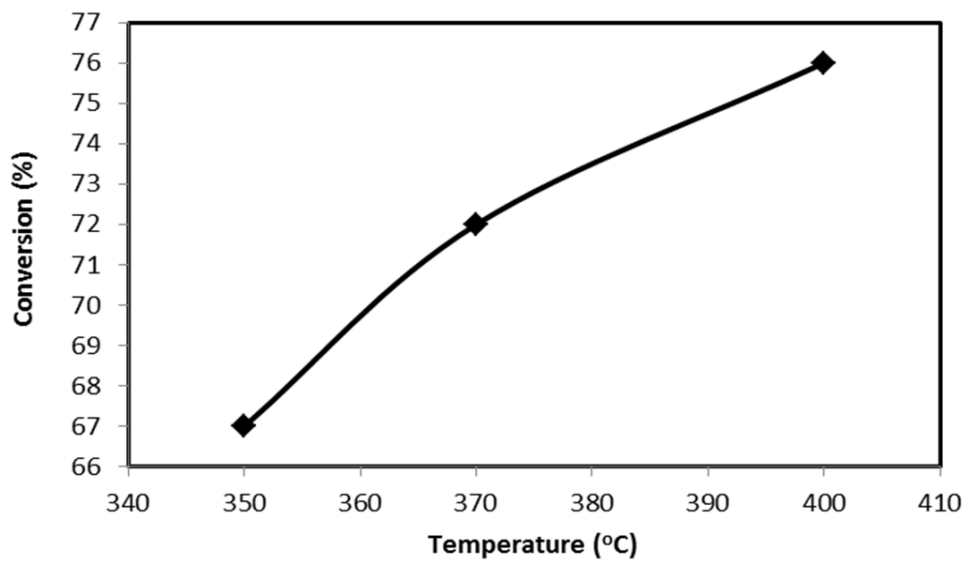


Figure 42 Conversion vs Temperature for Template coating (SAPO-34/SiC-T)

### **1.20.2 Comparison of the Dehydration Activities of SAPO-34/SiC Composite and SAPO-34 Powder**

The dehydration activity of the supported SAPO-34 was also compared with that of the unsupported ones and the results are presented in Figure 43. For the accuracy of the comparison the weight of the zeolite in both catalysts was similar. The reaction was carried out at a relatively low space velocity ( $1000 \text{ h}^{-1}$ ) in order to reduce the artifact linked with the pressure drop through the powder zeolite. According to the results the two catalysts exhibited similar dehydration performance and stability during the test. The results indicated that supported SAPO-34 with macroscopic shaping not only displays advantages such as controlled macroscopic shaping, low pressure drop, easy handling and transport but also high catalytic activity for the dehydration process. In addition, the supported zeolite displayed a slightly higher selectivity towards DME than the unsupported ones, i.e. 96 instead of 94%. The slight improvement of the DME selectivity could be attributed to the high escaping rate of the intermediate DME from the supported zeolite layer coated on the SiC foam surface.

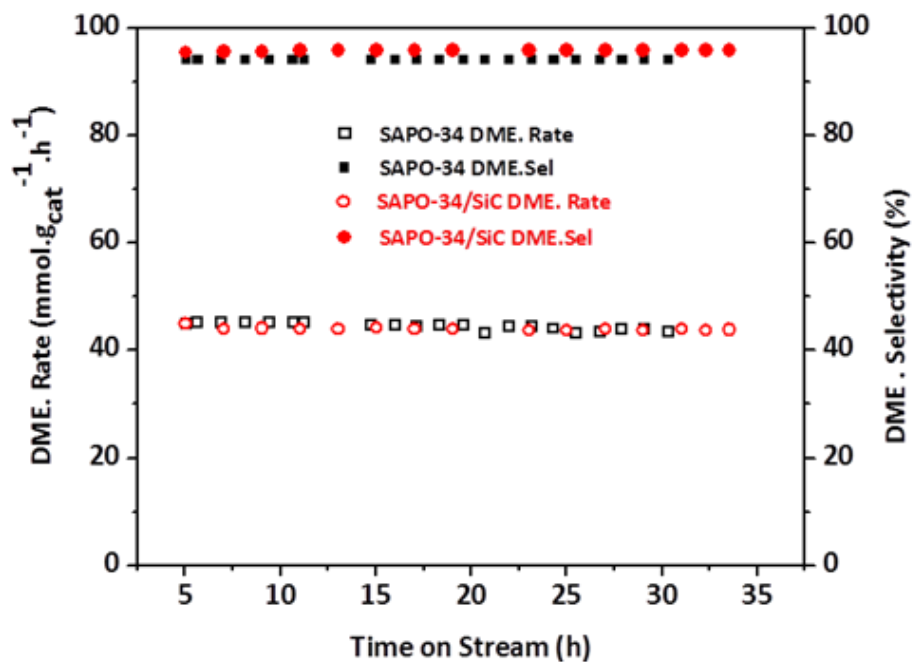


Figure 43 Dehydration Activity and DME Selectivity on the SAPO-34/SiC and SAPO-34 Catalysts in a Fixed-bed Reactor, Reaction Conditions: Weight of SAPO-34 = 150 mg, Reaction Temperature = 370 °C, Atmospheric Pressure, CH<sub>3</sub>OH Concentration = 25 vol. %, Gaseous Hourly Space Velocity (GHSV) = 1000 h<sup>-1</sup>

## CHAPTER 6

### CONCLUSIONS AND RECOMMENDATIONS

In this chapter a conclusion of this master thesis will be presented followed by recommendations for future work.

#### 1.21 SAPO-34 Purity Studies

The following points represent the summary of the SAPO-34 phase purity investigations that was conducted using both hydrothermal and microwave assisted synthesis methods.

Regarding the hydrothermal synthesis route, pure SAPO-34 can only be obtained at  $\text{SiO}_2/\text{Al}_2\text{O}_3$  ratios greater than 0.3, whereas the template concentrations was crucial for the synthesis of pure SAPO-34 which was obtained at relatively high template concentrations. However, all the syntheses with different dilution ratios produced pure crystalline SAPO-34 molecular sieve, with water ratio of 110 exhibited the higher crystallinity.

As far as the microwave assisted synthesis method is concerned, pure SAPO-34 was produced at shorter duration (6 h microwave irradiation) as compared to 24 h in the hydrothermal synthesis method. Furthermore, higher crystallinity was observed in samples prepared with microwave method. In addition to the visibility of synthesizing low content pure SAPO-34 ( $\text{SiO}_2/\text{Al}_2\text{O}_3$  lower than 0.3).

In general, SAPO-18 co-crystallized with SAPO-34 when the hydrothermal synthesis method was used, and SAPO-5 was the competing phase when microwave mediated synthesis was applied.

## **1.22 Fabrication of the SAPO-34/SiC Foam Composite**

All the attempts to grow SAPO-34 on SiC foam via conventional heating method failed due to the attachment of the co-precipitated powders on the foam surface. However, we have succeeded to perform microwaves synthesis of SAPO-34 on the SiC foam structure.

The increase in the microwave irradiation duration in the synthesis of SAPO-34/SiC foam composites did not affect the crystal size but rather improved the homogeneity of crystal growth. Moreover, multi-coating steps were required in order to achieve full coverage of SAPO-34 crystals on the substrate surface.

In summary, the high amount of SAPO-34 can be loaded on to the SiC foam surface through template pre-impregnation process which allows one to reduce in a significant manner the inactive weight of the support per unit volume of the reactor without excessive pressure drop across the catalytic bed. The SiO<sub>2</sub> layer presents on the SiC surface provides a strong anchorage interface for the subsequence growth of the zeolite resulting to a high mechanical strength of the final composite for further handling and processing.

### **1.23 Catalytic Dehydration of Methanol to DME**

The as-synthesized catalyst exhibits a relatively high dehydration activity even at a high space velocity,  $4500 \text{ h}^{-1}$ , along with a high stability as almost no deactivation was observed as a function of time on stream.

The supported catalyst exhibits a similar dehydration activity compared to the unsupported ones under the same reaction conditions which indicates that the supported zeolite displays the same intrinsic activity compared to the powder zeolite.

## 1.24 Recommendations and Future Work

The following points are some recommendations for possible research areas for future investigations:

- Applying alkali pretreatments for the support material.
- Control the crystals orientation to improve the catalytic performance.
- Check the dehydration activity with other reaction conditions, i.e. zeolite loading, space velocity, methanol concentration, SiC foam window size and macroscopic shape.
- Studying the influence of the methanol purity, i.e. water concentration, on the dehydration performance and stability.
- The use of such hybrid catalyst in other applications where composites with open structure and high effective surface area are key issues.

## REFERENCES

- [1] Jacobs P, Flanigen E, Jansen J, van Bekkum H. Introduction to zeolite science and practice: Elsevier; 2001.
- [2] Barrer RM. Separations using zeolitic materials. *Discussions of the Faraday Society*. 1949;7:135-41.
- [3] Sherman JD. Synthetic zeolites and other microporous oxide molecular sieves. *Proceedings of the National Academy of Sciences*. 1999;96:3471-8.
- [4] Nicholas CP. Overview and Recent Developments in Catalytic Applications of Zeolites. *Zeolites in Industrial Separation and Catalysis*. 2011:355-402.
- [5] Lok BM, Messina CA, Patton RL, Gajek RT, Cannan TR, Flanigen EM. Silicoaluminophosphate molecular sieves: another new class of microporous crystalline inorganic solids. *Journal of the American Chemical Society*. 1984;106:6092-3.
- [6] Medvecký L, Mihalik J, Briančin J. Possibilities of coating of glass with synthetic zeolites. *Journal of Materials Science Letters*. 1993;12:907-9.
- [7] Izadbakhsh A, Farhadi F, Khorasheh F, Sahebdeifar S, Asadi M, Feng YZ. Effect of SAPO-34's composition on its physico-chemical properties and deactivation in MTO process. *Applied Catalysis A: General*. 2009;364:48-56.
- [8] Chen D, Moljord K, Fuglerud T, Holmen A. The effect of crystal size of SAPO-34 on the selectivity and deactivation of the MTO reaction. *Microporous and Mesoporous Materials*. 1999;29:191-203.
- [9] Kim H-S, Lee S-G, Kim Y-H, Lee D-H, Lee J-B, Park C-S. Improvement of lifetime using transition metal-incorporated SAPO-34 nano catalysts in conversion of dimethyl ether to light olefins.
- [10] Razavian M, Halladj R, Askari S. Recent advances in silicoaluminophosphate nanocatalysts synthesis techniques and their effects on particle size distribution. *Rev Adv Mater Sci*. 2011;29:83-99.
- [11] Deshayes S, Liagre M, Loupy A, Luche J-L, Petit A. Microwave activation in phase transfer catalysis. *Tetrahedron*. 1999;55:10851-70.

- [12] Kappe CO. Controlled microwave heating in modern organic synthesis. *Angewandte Chemie International Edition*. 2004;43:6250-84.
- [13] Liu X, Du S, Zhang B. The seeded growth of dense and thin SAPO-34 membranes on porous  $\alpha$ -Al<sub>2</sub>O<sub>3</sub> substrates under microwave irradiation. *Materials Letters*. 2013;91:195-7.
- [14] Girnus I, Pohl MM, Richter-Mendau J, Schneider M, Noack M, Venzke D, et al. Synthesis of AlPO<sub>4</sub>-5 aluminumphosphate molecular sieve crystals for membrane applications by microwave heating. *Advanced Materials*. 1995;7:711-4.
- [15] Li Y, Yang W. Microwave synthesis of zeolite membranes: a review. *Journal of Membrane Science*. 2008;316:3-17.
- [16] Yan Y, Davis ME, Gavalas GR. Preparation of zeolite ZSM-5 membranes by in-situ crystallization on porous  $\alpha$ -Al<sub>2</sub>O<sub>3</sub>. *Industrial and Engineering Chemistry Research*. 1995;34:1652-61.
- [17] Dong WY, Ren Y, Long YC. In-situ synthesis of B-Al-MFI-type zeolite membrane on a porous glass disc by substrate self-transformation. *Acta Chimica Sinica*. 2000;58:1311-5.
- [18] Wang Z, Yan Y. Oriented zeolite MFI monolayer films on metal substrates by in situ crystallization. *Microporous and Mesoporous Materials*. 2001;48:229-38.
- [19] Li G, Kikuchi E, Matsukata M. The control of phase and orientation in zeolite membranes by the secondary growth method. *Microporous and Mesoporous Materials*. 2003;62:211-20.
- [20] Huang A, Lin YS, Yang W. Synthesis and properties of A-type zeolite membranes by secondary growth method with vacuum seeding. *Journal of Membrane Science*. 2004;245:41-51.
- [21] Yilmaz B, Shattuck KG, Warzywoda J, Sacco Jr A. Oriented growth of ETS-4 films using the method of secondary growth. *Chemistry of Materials*. 2006;18:1107-12.
- [22] Jansen J, Koegler J, Van Bekkum H, Calis H, Van Den Bleek C, Kapteijn F, et al. Zeolitic coatings and their potential use in catalysis. *Microporous and mesoporous materials*. 1998;21:213-26.
- [23] Yang G, Zhang X, Liu S, Yeung KL, Wang J. A novel method for the assembly of nano-zeolite crystals on porous stainless steel microchannel and then zeolite film growth. *Journal of Physics and Chemistry of Solids*. 2007;68:26-31.

- [24] Bonaccorsi L, Proverbio E. Synthesis of thick zeolite 4A coatings on stainless steel. *Microporous and Mesoporous Materials*. 2004;74:221-9.
- [25] Wang Y, Tang Y, Wang X, Shan W, Ke C, Gao Z, et al. Fabrication of zeolite coatings on stainless steel grids. *Journal of Materials Science Letters*. 2001;20:2091-4.
- [26] Grande CA, Cavenati S, Barcia P, Hammer J, Fritz HG, Rodrigues AE. Adsorption of propane and propylene in zeolite 4A honeycomb monolith. *Chemical Engineering Science*. 2006;61:3053-67.
- [27] Zamaro JM, Ulla MA, Miró EE. Zeolite washcoating onto cordierite honeycomb reactors for environmental applications. *Chemical Engineering Journal*. 2005;106:25-33.
- [28] Buciuman F-C, Kraushaar-Czarnetzki B. Preparation and characterization of ceramic foam supported nanocrystalline zeolite catalysts. *Catalysis Today*. 2001;69:337-42.
- [29] Seijger GBF, Oudshoorn OL, van Kooten WEJ, Jansen JC, van Bekkum H, van den Bleek CM, et al. In situ synthesis of binderless ZSM-5 zeolitic coatings on ceramic foam supports. *Microporous and Mesoporous Materials*. 2000;39:195-204.
- [30] Patcas FC. The methanol-to-olefins conversion over zeolite-coated ceramic foams. *Journal of Catalysis*. 2005;231:194-200.
- [31] Coronas J, Santamaria J. The use of zeolite films in small-scale and micro-scale applications. *Chemical engineering science*. 2004;59:4879-85.
- [32] Gu L, Ma D, Yao S, Liu X, Han X, Shen W, et al. Template-Synthesized Porous Silicon Carbide as an Effective Host for Zeolite Catalysts. *Chemistry-A European Journal*. 2009;15:13449-55.
- [33] Seijger G, Oudshoorn O, Van Kooten W, Jansen J, Van Bekkum H, Van Den Bleek C, et al. In situ synthesis of binderless ZSM-5 zeolitic coatings on ceramic foam supports. *Microporous and Mesoporous Materials*. 2000;39:195-204.
- [34] Winé G, Tessonnier J-P, Rigolet S, Marichal C, Ledoux M-J, Pham-Huu C. Beta zeolite supported on a  $\beta$ -SiC foam monolith: A diffusionless catalyst for fixed-bed Friedel-Crafts reactions. *Journal of Molecular Catalysis A: Chemical*. 2006;248:113-20.

- [35] Yilai J, Zhenming Y, Xiaoming C, Chong T, Yong G, Jinsong Z. In Situ Synthesis of Silicalite-1 Type Zeolite on SiC Foam Ceramics. *Rare Metal Materials and Engineering*. 2009;38:286-8.
- [36] Jiao Y, Jiang C, Yang Z, Zhang J. Controllable synthesis of ZSM-5 coatings on SiC foam support for MTP application. *Microporous and Mesoporous Materials*. 2012;162:152-8.
- [37] Geus ER, Den Exter MJ, van Bekkum H. Synthesis and characterization of zeolite (MFI) membranes on porous ceramic supports. *Journal of the Chemical Society, Faraday Transactions*. 1992;88:3101-9.
- [38] Zhu J, Fan Y, Xu N. Modified dip-coating method for preparation of pinhole-free ceramic membranes. *Journal of Membrane Science*. 2011;367:14-20.
- [39] Soulages NL, Brieva AM. Gas chromatographic determination of the paraffin and naphthene content in saturated hydrocarbon distillates with porous layer open tubular columns of molecular sieve 13X. *Journal of Chromatography A*. 1974;101:365-71.
- [40] Schneider W, Frohne JC, Bruderreck H. Determination of hydrocarbons in the parts per 10<sup>9</sup> range using glass capillary columns coated with aluminium oxide. *Journal of Chromatography A*. 1978;155:311-27.
- [41] Rane N, Zou H, Buelna G, Lin JYS. Sol-gel synthesis and properties of unsupported and supported mesoporous ceria membranes. *Journal of Membrane Science*. 2005;256:89-97.
- [42] Perdana I, Creaser D, Made Bendiyasa I, Rochmadi, Wikan Tyoso B. Modelling adsorption in a thin NaZSM-5 film supported on a cordierite monolith. *Chemical Engineering Science*. 2007;62:3882-93.
- [43] Yao J, Zeng C, Zhang L, Xu N. Vapor phase transport synthesis of SAPO-34 films on cordierite honeycombs. *Materials Chemistry and Physics*. 2008;112:637-40.
- [44] Ivanova S, Vanhaecke E, Dreibine L, Louis B, Pham C, Pham-Huu C. Binderless HZSM-5 coating on  $\beta$ -SiC for different alcohols dehydration. *Applied Catalysis A: General*. 2009;359:151-7.
- [45] Louis B, Ocampo F, Yun HS, Tessonnier JP, Pereira MM. Hierarchical pore ZSM-5 zeolite structures: From micro- to macro-engineering of structured catalysts. *Chemical Engineering Journal*. 2010;161:397-402.

- [46] Lixiong Z, Mengdong J, Enze M. Synthesis of SAPO-34/ceramic composite membranes. *Studies in Surface Science and Catalysis*. 1997;105:2211-6.
- [47] Gu L, Ma D, Hu G, Wu J, Wang H, Sun C, et al. Fabrication and catalytic tests of MCM-22/silicon carbide structured catalysts. *Dalton Transactions*. 2010;39:9705-10.
- [48] Louis B, Tezel C, Kiwi-Minsker L, Renken A. Synthesis of structured filamentous zeolite materials via ZSM-5 coatings of glass fibrous supports. *Catalysis today*. 2001;69:365-70.
- [49] Zhao T-S, Takemoto T, Tsubaki N. Direct synthesis of propylene and light olefins from dimethyl ether catalyzed by modified H-ZSM-5. *Catalysis Communications*. 2006;7:647-50.
- [50] Feng D, ZUO Y, WANG D, WANG J. Steam reforming of dimethyl ether over coupled ZSM-5 and Cu-Zn-based catalysts. *Chinese Journal of Catalysis*. 2009;30:223-9.
- [51] Fu Y, Hong T, Chen J, Auroux A, Shen J. Surface acidity and the dehydration of methanol to dimethyl ether. *Thermochimica Acta*. 2005;434:22-6.
- [52] Spivey JJ. Review: Dehydration Catalysts For The Methanol/Dimethyl Ether Reaction. *Chemical Engineering Communications*. 1991;110:123-42.
- [53] Bandiera J, Naccache C. Kinetics of methanol dehydration on dealuminated H-mordenite: Model with acid and basic active centres. *Applied catalysis*. 1991;69:139-48.
- [54] Kim SD, Baek SC, Lee Y-J, Jun K-W, Kim MJ, Yoo IS. Effect of  $\gamma$ -alumina content on catalytic performance of modified ZSM-5 for dehydration of crude methanol to dimethyl ether. *Applied Catalysis A: General*. 2006;309:139-43.
- [55] Khandan N, Kazemeini M, Aghaziarati M. Determining an optimum catalyst for liquid-phase dehydration of methanol to dimethyl ether. *Applied Catalysis A: General*. 2008;349:6-12.
- [56] Yaripour F, Baghaei F, Schmidt I, Perregaard J. Synthesis of dimethyl ether from methanol over aluminium phosphate and silica-titania catalysts. *Catalysis Communications*. 2005;6:542-9.

- [57] Lertjiamratn K, Prasertdam P, Arai M, Panpranot J. Modification of acid properties and catalytic properties of AlPO<sub>4</sub> by hydrothermal pretreatment for methanol dehydration to dimethyl ether. *Applied Catalysis A: General*. 2010;378:119-23.
- [58] Dai W, Kong W, Wu G, Li N, Li L, Guan N. Catalytic dehydration of methanol to dimethyl ether over aluminophosphate and silico-aluminophosphate molecular sieves. *Catalysis Communications*. 2011;12:535-8.
- [59] Pop G, Bozga G, Ganea R, Natu N. Methanol conversion to dimethyl ether over H-SAPO-34 catalyst. *Industrial & Engineering Chemistry Research*. 2009;48:7065-71.
- [60] Lu W-Z, Teng L-H, Xiao W-D. Simulation and experiment study of dimethyl ether synthesis from syngas in a fluidized-bed reactor. *Chemical Engineering Science*. 2004;59:5455-64.
- [61] Fukahori S, Koga H, Kitaoka T, Nakamura M, Wariishi H. Steam reforming behavior of methanol using paper-structured catalysts: Experimental and computational fluid dynamic analysis. *International Journal of Hydrogen Energy*. 2008;33:1661-70.
- [62] Ivanova S, Vanhaecke E, Louis B, Libs S, Ledoux MJ, Rigolet S, et al. Efficient Synthesis of Dimethyl Ether over HZSM-5 Supported on Medium-Surface-Area  $\beta$ -SiC Foam. *ChemSusChem*. 2008;1:851-7.
- [63] Liu Y, Podila S, Nguyen DL, Edouard D, Nguyen P, Pham C, et al. Methanol dehydration to dimethyl ether in a platelet milli-reactor filled with H-ZSM5/SiC foam catalyst. *Applied Catalysis A: General*. 2011;409:113-21.
- [64] Emrani P, Fatemi S, Talesh SA. Effect of Synthesis Parameters on Phase Purity, Crystallinity and Particle Size of SAPO-34. *IRANIAN JOURNAL OF CHEMISTRY AND CHEMICAL ENGINEERING (IJCCE)*. 2011.
- [65] Strohmaier KG. Synthesis of molecular sieves of CHA framework type. *Google Patents*; 2004.
- [66] Vomscheid R, Briend M, Peltre M, Man P, Barthomeuf D. The role of the template in directing the Si distribution in SAPO zeolites. *The Journal of Physical Chemistry*. 1994;98:9614-8.
- [67] Bonaccorsi L, Calabrese L, Freni A, Proverbio E. Hydrothermal and microwave synthesis of SAPO (CHA) zeolites on aluminium foams for heat pumping applications. *Microporous and Mesoporous Materials*. 2013;167:30-7.

- [68] Li Y-G, Yong S, Weizhong J, Changgeng P. A novel route of synthesis of ZSM-5 zeolite membranes. *Materials Letters*. 1998;37:221-6.
- [69] Calis HPA, Jansen JC, Oudshoorn OL, Van BH, Van DPN. Method for preparing a composite catalyst. *Google Patents*; 1998.



## **Publications**

- Microwave Assisted Growth of SAPO-34 on  $\beta$ -SiC Foams for Methanol Dehydration to Dimethyl Ether (Submitted to Journal of Materials Chemistry A, I.F=6.1).
- Methanol Dehydration to DME over SAPO-34/SiC foam structured catalyst (Written).
- SAPO-34 Grown on SiC Foams for DME to Olefins (under preparation).
- Isothermal Vapor Liquid Equilibrium for 1,1-difluoroethane (HFC-152a) and n-butane (R-600) (under preparation).

## **Conferences**

- Controlled growth of SAPO-34 on SiC foams, 6<sup>th</sup> International Zeolite Membrane Meeting, 2013, Korea.
- Microwave Assisted Growth of SAPO-34 on  $\beta$ -SiC Foams for Methanol Dehydration to Dimethyl Ether, Federal European Zeolite Association (FEZA) Conference, Germany, Leipzig, October 2014.

## **Projects**

- Ms. Thesis project titled (Silicoaluminophosphate, SAPO-34 Grown on Solid Foams as Structured Catalysts and their Application in Methanol to Olefin Process) (Funded by NSTIP, Project No. 11-NAN2166-04 ).
- Modeling of Vapor Liquid Equilibrium of Refrigerants Mixtures Using MATHEMATICA.
- 5<sup>th</sup> year graduation project titled (Design of a Gas Condensate Field Production Facility), Advisor: Dr. Ali Rabah, CHE Department, University of Khartoum.

- 4<sup>th</sup> year project titled (Economic Evaluation of Shifting Refinery Products from Fuels to LPG and other Feedstocks for Petrochemical Industry), Advisor: Dr. Ali Rabah, CHE Department, University of Khartoum.

## **Work Experiences**

October 2010 – January 2 Teaching Assistant, Chemical Engineering Department, University of Khartoum

## **Training**

September, 2009: Short course about Nanotechnology, International Islamic University Malaysia, IIUM.

## **References**

1. Dr. Ibelwaleed Ali Hussein, Professor, Department of Chemical Engineering, King Fahd University of Petroleum and Minerals.  
Tel. (03) 860-2235, e-mail: [ihussein@kfupm.edu.sa](mailto:ihussein@kfupm.edu.sa)
2. Dr. Oki Muraza, Assistant Professor, Department of Chemical Engineering and Center of Research Excellence in NanoTechnology (CENT), King Fahd University of Petroleum and Minerals.  
Bld 15-3012 PO Box 5040 Dhahran 31261 KSA  
<http://faculty.kfupm.edu.sa/CHE/omuraza/>  
Email: [omuraza@kfupm.edu.sa](mailto:omuraza@kfupm.edu.sa)  
Mobile: +966 54 587 3454
3. Dr. Ali A. Rabbah, Head of Chemical Engineering Department, University of Khartoum.  
Mobile: (+249) 0912883212